Reviewers' comments:

Reviewer #1 (Remarks to the Author):

In their paper, Capozzi et al. demonstrate an approach of quenching UV-induced radicals in a DNP process for producing hyperpolarized [U-13C, d7]-D-glucose, storing it in a solid radical-free hyperpolarized state, thus, allowing transport of the hyperpolarized sample from the point of production to a remote point of NMR detection. While the idea of generating and quenching UV-based radicals in the dDNP process (as well as the idea of transportable DNP-polarized agents) is not new, realization of the separation between the two steps of the process, i.e., hyperpolarization/quenching and detection, is demonstrated for the first time to the best of my knowledge. This was accomplished by solving a magnitude of "technicalities" which is, nonetheless, constitute a typical bottleneck in experimental science. In particular, it was discovered that implementing permanent magnets inside the DNP probe was necessary to "shelter" hyperpolarization during the sample extraction; otherwise, relaxation is too fast at low fields. The paper is very well written and polished. While some minor jargon is present throughout the paper, it will still be interesting for the hyperpolarized NMR community as it brings significant insights to this specialized area of research. I recommend publication in Communication Chemistry.

Reviewer #2 (Remarks to the Author):

In this work the authors nicely present a method to preserve the hyperpolarized state of metabolic contrast agents outside the polarization instrument. This is a major achievement that may lift a major barrier in metabolic hyperpolarized magnetic resonance research and allow other players to enter the field. The authors nicely discuss the achievements and the problems still to solve.
The technology is demonstrated on [U-13C, d7]-D-glucose, an agent with a relatively short lifetime compared to the main dDNP agent [1-13C]pyruvate and therefore more challenging.

I have reviewed the parts within my expertise. I am not an expert on magnetic field simulations or hardware design, including the design of NMR probes or permanent magnets. I would trust the authors on those due to their track record in designing and implementing such instrumentation and the level of detail given.

I only have minor comments as regards to the text.

Introduction
1. "characterized by high glucose uptake" is not clear in the context of this statement.
2. As regards to FDG-PET, please indicate more clearly the ionizing radiation to which patients are exposed to and the limitations on repeated examinations and use in certain patient populations.
3. "good spectral separation" – not clear
4. The authors place major focus on the comparability to FDG-PET operational considerations. In this regard:
a. FDG-PET uses a 2-deoxyglucose derivative, please indicate that the parallel agent to this in hyperpolarized MR would be a stable isotope labeled 2-deoxyglucose agent. Please cite DOI: 10.1038/s41598-019-56063-0 in this regard.
b. The first use of hyperpolarized [U-13C, d7]-D-glucose for MR imaging that parallels the FDG-PET examination (without metabolic pathway resolution) was reported several years ago and should be

cited, DOI: 10.1002/cmmi.1497.

Results
5. The section “A “make it all” device” is not results. I would move this to the Methods in a separate section on the Description of the system. The same goes for the 1st paragraph of the section “Hyperpolarized sample with extended lifetime”. The same goes for Figure 1 and Figure 6.

6. Movie S1 is important and well presented, maybe I missed it but how long did the transfer procedure take here actually? From the rest of the text (Discussion) it is not clear if the time to reach the dissolution site was 3 min or the dissolution procedure took 3 min from arrival to the dissolution site. I thought the latter as per the description in the Results but the paragraph starting with “A more potent source…” in the discussion confused me.

Discussion
7. What would be the role of the [U-13C, d7]-D-glucose formulation? The authors understandably use a formulation already used by this group. However, it should be noted that other formulations have been developed and studied for this agent (even if in a different magnetic field). For example, please see DOI: 10.1002/cphc.201900946.

8. Sentence starting with “Under these conditions, the T1 measured…” unclear.

Online methods
9. Dissolution: It is not clear why one would dissolve a glucose sample in a phosphate buffer as glucose is not acidic. The dissolution buffer appears hypo-osmotic and contains EDTA, both are likely to lead to prolonged T1 compared to solutions intended for biological use.

10. Enhancement calculation: 100 ms repetition time seems really short for 13C of glucose. Was this time enough for obtaining fully relaxed spectra? If not, is the T1 under these conditions known? Was the line-width affected by Gd doping? Could it be that this affected the polarization % that was determined?

11. Page 22: relaxion, correct

Reviewer #3 (Remarks to the Author):

The authors report a very important improvement to dDNP: the transfer of frozen samples with long T1. The present some modification to a DNP system that allows them to keep the sample at an elevated magnetic field to reduce relaxation losses. the sample is transfered to an NMR and detected. A few % polarization were observed on glucose.

This report is an essential progress that must be published.

Unfortunately, I have some issues with the scholary presentation of the work. I find many

superfluous sentences, colloquialisms, unclear structures on the one hand, and litte substantial data on the other (eg. on chemistry, its a chemistry journal after all). The abstract (which is not an abstract in my opinion) is even a bit missleading in suggesting that you solved the T1 issue of glucose. The short T1 in vivo remains the major issue which is not addressed at all (see paper by Rodrigues et al). You dont explicitly say that you did, but you don't deny either, and in the context is appears as such.

You will find many comments in the attached file, unclear language is highlighted.

Thus I strongly encourage the authors to revise this utterly important paper make to make it more matter-of-fact-style, to tone down many expessions and to give realistic assessement of Glucose. To be honest, I don't see Glucose going anywhere until T1 in vivo is longer, so it may not be the perfect molecule to demonstrate delivery of HP samples, but as a demonstrator its OK.

To be absolutely clear: this is an absolute breakthrough for DNP and must be published. But IMHO, please modify the way you present it.

Thanks for your efforts! its an important contribution to the field.

Metabolic contrast agents produced from transported solid ^{13}C-glucose hyperpolarized via Dynamic Nuclear Polarization

Andrea Capozzi,[1,2 *] Jan Kilund,[2] Magnus Karlsson,[2] Saket Patel,[2] Arthur Cesar Pinon,[2] Olivier Ouari,[3] Mathilde H. Lerche,[2] and Jan Henrik Ardenkjær-Larsen.[2]

[1] *LIFMET, Department of Physics, EPFL, Station 6 (Batiment CH), 1015 Lausanne (Switzerland)..*

[2] *HYPERMAG, Department of Health Technology, Technical University of Denmark, Building 349, 2800 Kgs Lyngby (Denmark).*

[3]*Institut de Chimie Radicalire Aix-Marseille Université, CNRS, ICR UMR 7273, 13397 Marseille Cedex 20 (France).*

Corresponding author

*Dr. Andrea Capozzi

EPFL SB IPHYS LIFMET

CH F0 632 (Bâtiment CH)

Station 6

CH-1015 Lausanne

T: +41 21 693 05 88

Email: andrea.capozzi@epfl.ch

ORCID: 0000-0002-2306-9049

Abstract

Hyperpolarized (HP) ^{13}C-labelled metabolic contrast agents (MCAs) via dissolution Dynamic Nuclear Polarization (dDNP) are generating significant interest for their ability to inform, non-invasively and in real-time, on tissue specific aberrant metabolism. However, an inherent short lifetime of these agents combined with demanding and expensive hyperpolarization equipment hamper the adoption of the method in the clinic. For these reasons, glucose metabolism for cancer diagnostic and treatment monitoring purposes is currently performed by means of ^{18}F-fluoro-deoxy-glucose (^{18}F-FDG) Positron Emission Tomography (PET) examinations. Nevertheless, this technique presents some limitations such as lack of specificity in organs with a high normal glucose uptake and use of ionizing radiation.

In this work, we present a paradigm shift in the dDNP technique built on photo-induced thermally labile radicals, which allow solid sample extraction from the dDNP polarizer and hours long lifetime of the MCAs. We demonstrate the ability to disconnect elaborate equipment to produce above 10,000-fold signal enhanced MCAs, [U-^{13}C, d_7]-D-glucose, from its end-user site, enabled by HP sample storage and transport. Such remote production of ^{13}C-labelled MCAs, with hours long lifetime at appropriate transport conditions, would be much like the way ^{18}F-FDG PET is currently performed in the clinic.

Introduction

Changes in metabolic pathways, causal of the origin or progression of diseases such as cancer, diabetes and neurodegenerative diseases can be studied non-invasively with metabolic imaging methods.[1–3] The latter are thus powerful means to diagnose and monitor response to therapy.[4] Despite significant research progress, methods used to measure metabolism in patients are still limited and blind to many cellular processes.[5]

Among those, ^{18}F-fluoro-deoxy-glucose positron emission tomography (^{18}F-FDG PET) is the current benchmark to assess hypo- or hypermetabolism in clinical practice, in particular for what concerns cancer diagnosis, staging, and treatment monitoring.[6] Nevertheless, ^{18}F-FDG PET has its limitations. For instance, it suffers from poor specificity in organs with a high normal glucose uptake;[7] non-cancerous inflammations, characterized by high glucose uptake, can result in false positives;[8] the radioactive nature of the tracer exposes the patient to potentially dangerous ionizing radiations. Most of all, the information obtained is limited to glucose uptake since downstream metabolites like lactate and tricarboxylic acid (TCA) cycle intermediates are invisible to the technique.[9,10]

A more direct and specific way to track metabolism in vivo is to follow the fate of exogenous substrates by ^{13}C magnetic resonance spectroscopy (MRS) or spectroscopic imaging (MRSI). These techniques allow phenotypical characterization of tumors by looking at downstream metabolism enabled by good spectral separation of the different metabolites.[10] However, ^{13}C-MRS and MRSI widespread use in the clinic is limited by low sensitivity. The MR signal is proportional to the nuclear spin concentration and nuclear spin alignment (i.e. polarization) with respect to the applied magnetic field. Both features are limited in this kind of experiments. Signal averaging is the typical workaround to overcome low sensitivity. Unfortunately, the price to pay is poor temporal resolution and thus access to the highly informative metabolic flux.[11]

Deuterium metabolic imaging, a novel, noninvasive method, combines deuterium magnetic resonance spectroscopic imaging with oral intake or intravenous infusion of 6,6-^{2}H-labeled glucose to generate three-dimensional metabolic maps.[12] Although straightforward to implement, this technique is challenged by poor metabolite separation at clinical magnetic field strengths.

General advancement of MRS techniques comes from recent developments in hyperpolarization technologies.[13] Using hyperpolarized agents, the low sensitivity drawback of ^{13}C-MRS can be largely circumvented,[14] and metabolic activity can be imaged non-invasively and in real-time in humans.[15,16]

Dissolution dynamic nuclear polarization (dDNP) is the most versatile among the hyperpolarization methods.[17] With dDNP, hyperpolarized (HP) metabolic contrast agents (MCAs) can be obtained with ^{13}C-nuclear spin polarization up to 100.000-fold compared to thermal equilibrium on a clinical scanner.[18] The MCAs are produced in an expensive and technically demanding device called dDNP polarizer. The polarizer provides the appropriate conditions of temperature and magnetic field to transfer polarization from unpaired electron spins, added to the sample in form of organic radicals, to ^{13}C nuclear spins in the MCA, by using microwave irradiation. Unfortunately, dDNP is characterized by a striking unbalance between sample throughput and lifetime of the HP state. It typically takes hours to create a single injectable dose of MCA, whereas, after dissolution and extraction from the polarizer, the HP MCA's lifetime is only minutes in the best case. Currently, to equip an MR facility with hyperpolarization, the dDNP device must be located in near proximity to the scanner. Although dDNP HP ^{13}C-MRS has the potential to revolutionize diagnostic radiology enabling precision medicine and personalized healthcare,[15,19–21] this limitation threatens its development into widespread clinical use.

The ^{13}C polarization's half-life within the MCAs is several orders of magnitude longer when kept frozen at cryogenic temperature. This allows, in principle, transportation of the MCAs far away

from their production site.[22] Unfortunately, a dDNP sample cannot be extracted as a frozen solid without losing its hyperpolarization.[17,23] The problem is the paramagnetism of the radicals that are added to the sample to allow the DNP process to take place inside the polarizer.[24] Indeed, in solid samples doped with radicals, the nuclear spins relaxation becomes prohibitively fast at low magnetic field.[25] These are the conditions experienced by an HP sample when lifted far away from the high field of the DNP machine.[22,26,27] This is the reason why, to keep the MCA's hyperpolarization alive during sample extraction, the original dDNP technique requires the dissolution to be performed inside the polarizer at high field.[17]

To dispense of the presence of technically demanding and costly hardware at individual clinical sites, and instead hyperpolarize MCAs at a central facility for subsequent storage and distribution would demand a radically new way of producing HP MCAs. Such remote production of ^{13}C-labelled MCAs would be much like the way clinical examinations are performed with ^{18}F-FDG PET, where the tracer is delivered on demand.

The two key challenges to address are to extract the MCA as a frozen solid from the polarizer, while preserving its hyperpolarization, and to prolong the ^{13}C HP signal lifetime as much as possible under sample transport conditions. Three different concepts have been published for producing long-lasting HP samples for storage and transportation.[26–28] The critical point in these concepts is the absence or drastic reduction of paramagnetic relaxation during extraction from the polarizer of the sample still in the solid-state.

The first approach, proposed by Hirsch et al., does not use DNP. Thus, no paramagnetic agents are added to the MCA formulation, which is hyperpolarized by brute force (e.g. cooling down the sample to very low temperatures while keeping it at high magnetic field).[26] Although an easy solution to get rid of detrimental paramagnetism, this method is very slow (i.e. it takes tens of hours to thermally polarize the sample when working at 2 K and 14 T) and the obtained liquid-state hyperpolarization is between two and three orders of magnitude lower with respect to DNP.

The second approach, introduced by Ji et al., physically separates the radicals from the ^{13}C-MCA in the sample. DNP is performed on ^{1}H nuclei of a radical doped solvent that impregnates without dissolving the MCA. Then, ^{1}H -^{1}H spin diffusion and cross-polarization transfer the high spin order from solvent protons to ^{13}C nuclei borne on the MCA molecule.[27] This is an elegant idea for combining hyperpolarization via DNP to HP sample extraction and transportation. However, the distance between the ^{13}C nuclei and the radicals in the sample matrix makes the DNP process less efficient by a factor of three, at least.[27,29] Moreover, the radical-rich phase of the sample involves non-biocompatible solvents such as toluene and tetrahydrofuran.

The third approach hyperpolarizes the sample employing labile radicals originating from alpha keto acids UV-light irradiation. These radicals are stable at low temperature, where the DNP process takes place, but recombine into diamagnetic species above 190 K (i.e. the radical quenching temperature).[30–32] Therefore, a radical free HP solid sample can be obtained by heating the latter above the UV-radicals quenching temperature. Hyperpolarization of ^{13}C-MCAs using photo-induced non-persistent radicals has been optimized and shown to perform as good as DNP using stable radicals,[30,32,33] while employing endogenous/biocompatible substances only.

In 2017, Capozzi et al.[28] demonstrated in a proof-of-principle study that labile radicals for dDNP, generated via UV-irradiation of a sample containing a fraction of [1-^{13}C]pyruvic acid, could be quenched inside the polarizer by means of a “sample thermalization procedure”, while retaining most of the hyperpolarization obtained via DNP in the solid state. A dramatic increase of the ^{13}C T_1 was recorded after the removal of the radicals and this opened perspectives for solid sample storage. Unfortunately, lack of controlled sample extraction allowed no real attempt of transport.

In this work we exploit UV-induced radicals to generate highly polarized ^{13}C-MCAs in the liquid state with no need for dDNP polarizer on site. For the first time, we demonstrate transportation at cryogenic temperature of such samples. We establish a robust protocol for sample loading, polarization, thermalization, extraction, transport and dissolution away from the production site

of the HP ^{13}C-MCA solid sample. To this end we chose deuterated trimethylpyruvic acid (d_9-TriPA) as UV-radical precursor and [U-^{13}C, d_7]-D-glucose as substrate (30), the latter being a molecule showing increasing interest in the hyperpolarization community thanks to the richer metabolic pathways it can give access to, compared to routinely used [1-^{13}C]pyruvate.[34–36]

Specific hardware development allowed us to solve two stringent physics problems: 1) efficient heating of the sample while retaining most of the polarization; 2) avoid fast spin lattice relaxation at low-field present even in absence of radicals. We implemented a custom designed fluid path (CFP) with the purpose of diagnosing and solving experimental challenges as well as making it possible to run all steps of the experiment in a user-friendly closed system.

Results

A "make it all" device

Our first aim in this study was to build a device that could allow us to investigate, in a robust and reproducible way, all steps involved in a "remote DNP" experiment employing UV-induced radicals: UV-irradiated sample loading into the dDNP polarizer while keeping it below the critical temperature of around 190 K, hyperpolarization of the sample, UV-radicals elimination, HP sample extraction from the polarizer, HP sample storage and transport and finally HP sample dissolution away from the production site. To this end, we developed what we call a "custom designed fluid-path" (CFP). The device is reported in Fig. 1. All technical details for the construction and operation of the CFP are described in *Methods*. The threaded vial (parts 5 and 6 in Figure 1A), sealed to superfluid He by compressing a PTFE O-ring (part 12 in Figure 1D) allows loading solid samples through a 7 mm diameter opening. Moreover, this approach makes the CFP reusable as far as the O-ring is replaced after each experiment. The top part of the device is equipped with a quick release connector (part 1 in Figure 1A). This component made it possible to both quench the radicals and later dissolve the sample by injecting He gas or hot solvent inside the CFP, respectively. Moreover, the quick release helped transportability of the

CFP. Indeed, the CFP could be easily moved from the sample loading/leak-test station (see ref. [32,37] and Figure S1 for details) to the polarizer and finally into the storage/transport unit. The dynamic sealing (see Figure 1C) allowed us to operate the polarizer at low pressure (1 – 20 mbar range) during all the experiment's steps. Moreover, it was an asset when investigating the sample's relaxation properties, with and without radicals, at different distances from the superconductive magnet's isocenter, while keeping the base temperature unchanged. Most importantly, our aim was to deliver to the final user a compact "plug and play" solution to obtain the MCA in the liquid state on site: a CFP inside an appropriate transportation device.

Hyperpolarized sample with extended lifetime

In order to generate a radical free HP sample, we designed a specific experimental procedure involving the hardware earlier described. To this end, we used one single sample preparation consisting in 2.2 M of [U-^{13}C,d_7]-D-glucose dissolved in 60 µL of glycerol:water 1:1 (v/v). The d_9-TriPA was added in amount corresponding to 10% of the final volume to generate 40±4 mM or radical after UV-light irradiation (see *Methods* for details about sample preparation). The preparation and polarization of the sample was developed and optimized in a former publication.[30] Figure 2 shows the different steps and the NMR signal time course of a typical hyperpolarization experiment followed by radical quenching. DNP was performed at 6.7 T and 1.20±0.05 K using a dDNP polarizer (Magnet and cryostat from Magnex Scientific Ltd, Yarnton, UK) conceptually similar to the idea introduced in 2003,[17] but equipped with a sample loading chamber/air-lock module and a gate valve to be compatible with the fluid path technology.[38,39]

Figure 2A and the green portion of Figure 2D report the first part of the experiment: the sample vial was lowered into the NMR coil, microwave irradiation was performed at optimal conditions (see *Methods* for details), the sample reached a solid-state ^{13}C polarization of 45±5 % in approximately 1 h (buildup time constant 1300 ±10 s), in good agreement with our former study.[30] Then, the radical quenching procedure started.

Figure 2B and the yellow portion of Figure 2D illustrate this step: microwaves were switched off, the vial was lifted 15 cm above the NMR coil, outside the liquid He bath, and left there for 5 min; the CFP quick release was connected to a He gas line and the gas blown towards the sample.

Figure 2C and the orange portion of Figure 2D describe the last step of the experiment: the vial was moved back to the measurement position inside the NMR coil for checking the outcome of the radical quenching procedure. Firstly, NMR was acquired to evaluate the polarization loss during sample heating. Secondly, microwaves were switched ON again to verify the absence of any DNP process and qualitatively verify the quenching of the radicals. A quantitative check was performed later by extracting the CFP from the polarizer and recovering the beads from the sample vial into liquid nitrogen to measure any residual radical concentration by ESR (see *Methods*).

Radical scavenging parameters were optimized in a series of different experiments. The best result was found by blowing room temperature He gas for 20 s at 6 bar of pressure. This procedure allowed us to get rid of 99% of the radical in the sample (see Figure S2). At optimal conditions the polarization loss during the sample heating by means of He gas blowing was around 20% of the initial value. The inset in Figure 2D shows the "signature" of a successful thermalization experiment: the signal increased in the first few recorded NMR spectra.

Quenching of the radicals from the HP sample caused a dramatic increase of ^{13}C nuclear spin-lattice relaxation time. Figure 3 reports the signal evolution as a function of time, at 4.2 K and 6.7 T, in absence of microwave irradiation for a quenched sample (black circles) and a sample with the UV-radicals still present (blue circles). The ^{13}C T_1 increased from 2,300 ±20 s to 200,000±3,600 s (i.e. 55±1 h), confirming that the UV-radicals in the sample represented the main source of relaxation. We performed these measurements at 4.2 K instead of 1.2 K to better and more quickly visualize the T_1 difference between the two samples.

In a separate series of experiments, by implementing a manual field cycling inside the polarizer, we also measured the ^{13}C relaxation of a sample after UV-radicals quenching at 4.2 K and 1 T (see *Methods* for details about the field cycling implementation). In Figure S3 we report the results: by fitting the data to a mono-exponential curve, we found a T_1 of 4.0±0.5 h (R^2 = 0.97).

Minimal polarization loss during solid sample extraction

Unfortunately, the UV-radical quenching procedure alone was not enough to extract the sample from the DNP machine while retaining most of the polarization. In Figure 4A we outline the NMR signal intensity of two HP samples (one with UV-radicals still active and one after quenching) as a function of the polarizer's decreasing magnetic field along the z-axis. Thanks to the flexibility of the CFP dynamic sealing, the sample extraction path was recorded in steps of 10 cm from the magnet's isocenter to the loading chamber. For each step, the sample vial was lifted to the desired height, allowed to relax for 5 s and then lowered back to the measurement position inside the NMR coil. The first HP sample was not subjected to quenching before extraction (blue circles). In this case, a magnetic field of 350 mT (approx. 30 cm from the magnet's isocenter) was enough to cause a loss of almost half of the polarization created via DNP. Exposing the same sample to 100 mT (approx. 40 cm from magnet isocenter) caused an almost complete loss of polarization. The second HP sample was subjected to quenching before investigating the extraction. This sample could be exposed to a magnetic field as low as 40 mT (approx. 50 cm from magnet isocenter) while retaining most of the polarization. However, lower values of the magnetic field relaxed the polarization completely during the 5 s waiting time. The magnetic field profile of the superconductive magnet was measured with a Hall probe up to 3 T and simulated in MATLAB, according to the coil geometry, from 0 T to 6.7 T (see Figure S4). The simulation was in good agreement with the measured data points (R^2 = 0.98).

These results gave us useful information about how to modify the original DNP probe[40] to shelter the hyperpolarization of UV-radicals quenched samples during extraction. Accordingly, a

"magnetic rail" was designed using NdFeB permanent magnets along the path traveled by the sample. The starting point of the inserted magnets was chosen to be just below the position were the UV-radical quenched sample experienced its initial polarization loss (i.e. 40 cm above the magnet isocenter). The arrangements of the permanent magnets generated a field perpendicular to the one of the polarizer, and the value of the total field (from polarizer and permanent magnets) never dropped below 100 mT. To achieve this, we used four Halbach array arrangements, designed according to the probe geometry, to cover the space from 40 cm above the polarizer's isocenter to the loading chamber.

The additional field from the permanent magnets allowed us to move a thermalized sample from inside the NMR coil to the loading chamber, while retaining more than 90% of the polarization (see Figure 4B). The total magnetic field as a function of the distance from the magnet's isocenter is reported in Figure 4C. Details about the magnetic rail construction and magnetic field simulation are reported in the *Methods* section and Figure S5 and S6, respectively. Placing permanent magnets inside the DNP probe had no detrimental effects neither on the homogeneity or shift of the NMR resonance nor on the polarizer base temperature, despite potentially increased heat conductivity.

Successful sample transport and straightforward remote dissolution

Once we made sure we could freely move thermalized samples along the polarizer z-axis while retaining most of the polarization, we investigated and implemented transport and remote dissolution. From field cycling experiments inside the polarizer, it was clear that hours long T_1 could be obtained for [U-^{13}C, d_7]-D-glucose at 1 T and liquid helium temperatures (see above). Since storage in liquid helium requires a cryostat, we aimed instead at keeping the sample at liquid nitrogen temperature in a field of 1 T. The transport and remote dissolution procedure is outlined in Figure 5. The transport device was composed of two parts (see Figure 5A, B, C and D): a 300 mT four elements Halbach array magnetic guide at the top and a 1 T eight elements

Halbach array storage magnet at the bottom (see Figure S6 for details). The transport device was precooled to 77 K by placing it into a Styrofoam box filled with liquid nitrogen (see Figure 5E). The HP sample transport and remote dissolution entailed four main steps. Once the HP thermalized sample reached the loading chamber/air-lock, the polarizer's gate valve was closed, and the loading chamber/air-lock disconnected from the rest of the DNP probe. The loading chamber/air-lock was then docked to the transport device (Figure 5A and B), and the sample was pushed down into liquid nitrogen to reach the storage magnet (Figure 5C and D). The Styrofoam box was then put on a trolley, brought to a liquid state NMR laboratory installed two floors above the dDNP polarizer location, and the CFP connected to a compact dissolution station (see Figure S7) to extract the MCA in the liquid state. The HP MCA was finally injected into a 5 mm NMR tube and inserted in a 9.4 T vertical magnet to measure the polarization (see ref. 37 and *Methods* for details about the dissolution procedure).

The elapsed time between disconnection of the loading chamber/air-lock and remote dissolution was approx. 3 min. The glucose liquid-state polarization after dissolution was 4.0±1.0 %, (n = 4). One last optimization of the experiment was done by replacing the loading chamber/air-lock vacuum clamp with a quick release one, in order to speed-up its disconnection. This improved the measured ^{13}C liquid-state polarization to 9% (n = 1) (results reported in Figure 5F). We encourage the reader to watch the video recorded about the hyperpolarization transport and remote dissolution (see Movie S1).

Discussion

In this study, we exploited UV-induced labile radicals for DNP and smart hardware design to demonstrate, for the first-time, transport at cryogenic conditions and remote dissolution of HP [U-^{13}C, d_7]-D-glucose. The need to thoroughly understand nuclear relaxation phenomena as a function of temperature and field pushes us to develop a device, the CFP, able to cover all different steps of the experiment in a controlled way. The CFP turned out to be an extremely

293 useful device also for direct dissolution DNP experiments.[41,42] Implementation of permanent
294 magnets inside the DNP probe was a crucial step needed to successfully shelter the
295 hyperpolarization during sample extraction. In vision of a distribution of HP MCAs on a larger
296 scale, we envisage that several CFPs could be prepared by trained personnel and delivered on
297 demand.

298 At this stage of the study a careful evaluation of the polarization losses is important to suggest
299 further improvement of this technique as a game changer for production of transportable DNP
300 hyperpolarized MCAs.

301 As earlier reported,[30] a ^{13}C liquid-state glucose polarization of approx. 30% is obtained when the
302 sample formulation used in this study is dissolved directly from the dDNP polarizer (10 s interval
303 between dissolution onset and start of the NMR acquisition on the 9.4 T magnet, with a reported
304 [U-^{13}C, d_7]-D-glucose T_1 in solution of 20 s). When compared to our best result so far (^{13}C
305 polarization of 9% on a remote dissolved sample 3 min after sample extraction), we lose 2/3 of
306 the polarization during the extraction and transport process.

307 We characterized one source of relaxation in the experiment. The UV-radicals quenching process
308 accounts for a relative polarization loss of 20%. This would project the maximum achievable
309 liquid-state ^{13}C polarization for glucose to 24%, if dissolution occurred right after this step of the
310 experiment. According to the data reported in Figure 4B, lifting a UV-radical quenched sample to
311 the loading chamber causes almost no loss of polarization, as confirmed by the study from Ji et
312 al. for glucose embedded in a porous matrix and not in direct contact with the radicals.[27]
313 Moreover, if the gate valve was opened and the sample subjected to the cold He gas stream,
314 performing a fast extraction (10 s) compared to a slow one (approx. 2 min) did not make any
315 difference.

316 A more potent source of polarization loss is the unavoidable relaxation of HP glucose when kept
317 at 77 K and 1 T for the 3 min necessary to reach the site where the dissolution took place.

Unfortunately, we did not find in the literature T_1 data for glucose at such experimental conditions and, for the time being we do not dispose of the needed hardware to perform these measurements. We can, however, provide a rough estimation of the T_1 at these transport conditions (1 T, 77 K) by referring to data published by Hirsch et al. for solid [1-^{13}C]pyruvic acid, at 1.3 T and 60 K, with no radicals present in the sample.[43] Under these conditions, the T_1 measured over 5 min for a partially annealed pyruvic acid sample and remained constant down to 20 K,[43] where the methyl groups rotation is supposed to be minimal.[44] Assuming a similar value of T_1 for ~~our~~ sample at 1 T and 77 K, this would account for a relative polarization loss of approx. 50% during transport, projecting the maximum achievable liquid-state ^{13}C polarization value for glucose to 12 - 13%.

A third possible source of polarization loss could be the sample heating during the time interval needed to dock the loading chamber to the transportation device, when the He gas stream does not cool the sample anymore. The importance of this loss is supported by the improvement obtained by reducing the time to complete this operation by implementation of a quick release vacuum clamp.

To provide conditions for longer time storage and/or transport a colder environment is needed. At these experimental conditions, hours long T_1 can be obtained on ^{13}C-labelled small molecules, as previously demonstrated[43] and confirmed by our relaxation measurements of a thermalized [U-^{13}C, d_7]-D-glucose sample, where a T_1 of 4 h was obtained at 1 T and 4.2 K. Indeed, we are currently working on a more advanced transportable small bath cryostat able to work both at 4.2 K and 77 K and equipped with a 1 T Halbach magnet sufficiently homogenous to perform NMR on the HP sample extracted from the polarizer. This will allow a better estimation as well as reduction of the polarization losses.

An interesting observation in this study concerns the NMR signal profile just after the quenching procedure. As it is shown in the inset of Figure 2D, a good quenching procedure was

343 characterized by an increase of the signal just after plunging back the sample into the liquid
344 helium bath. Being the ^{13}C several order of magnitude above the thermal polarization level, we
345 ascribe this phenomenon to a temporary increase and subsequent stabilization of the NMR coil
346 Q-factor. Indeed, just after the quenching procedure the sample vial was "hot" and its insertion
347 into liquid helium generated a pressure increase into the VTI up to 20 mbar. This local heating
348 close to the NMR coil might decreases its Q-factor for the concerned time interval, resulting in a
349 slightly smaller detected NMR signal at the beginning of the acquisition.

350 Conversely, when the He gas did not bring enough heat to the sample to quench the radicals, the
351 effect described above was covered by a stronger initial decrease of the signal followed by a
352 plateau. This suggest that, in a Thermal Mixing interpretation of the phenomenon, the losses
353 during the thermalization process were due to thermal contact between the ^{13}C nuclear spins
354 reservoir and the ^{1}H nuclear spins reservoir mediated by the radicals non-Zeeman reservoir.[45–47]
355 Indeed, when heating up the sample, the protons relaxed very quickly due to efficient spin
356 diffusion (data not shown). If radicals are present in the sample, energy exchange may be
357 maintained between the different nuclear spin pools. In this case ^{1}H nuclei will "drain"
358 polarization from ^{13}C nuclei until the same spin temperature is achieved. Given that this
359 interpretation is correct, deuteration of the full sample matrix might help in reducing polarization
360 losses during the quenching procedure. Loss of polarization due to heating of the sample rather
361 than to a weaker magnetic field was supported by the fact that the sample vial could be kept for 5
362 min at 15 cm above the polarizer isocenter with no loss of polarization. This step was also useful
363 to gently increase the sample temperature and therefore facilitate the radical quenching
364 procedure. Moreover, during this process we chose to switch off the microwaves to avoid any
365 undesirable nuclear spin relaxation effect caused by microwaves propagation outside the cavity.[40]

366 It is worth noting that, with surprising reproducibility, 1% (i.e. 0.4 mM) of the initial radical
367 concentration was surviving the quenching process. This small amount of radicals did not
368 generate any particular problem during sample extraction from the polarizer when, as in this

study, the magnetic field is sufficiently high.[22] This observation, together with the evidence of no radical leftover in the liquid state,[30,31] suggests that the radical quenches in two steps: the main part at 190 K and the leftover at higher temperature.

Finally, we want to stress that the implementation of permanent magnets inside the DNP probe, generating a sufficiently high field, was crucial for successfully extracting the HP sample from the polarizer. Indeed, even in the ideal case of complete absence of paramagnetic impurities in the sample, for a magnetic field value < 40 mT ^{13}C and ^{1}H nuclei are subjected to "low-field thermal mixing".[22,27] When the Zeeman splitting difference between ^{1}H and ^{13}C nuclear spins is small compared to the width of the two resonance lines, energy can be exchanged between protons and carbons. Thus, if the ^{1}H spins' order is poor, due to relaxation during the thermalization process, polarization will be drained from ^{13}C spins until the two reservoirs achieve the same spin temperature. From the technical point of view, choosing permanent magnets that generate a magnetic field perpendicular to the polarizer's B_0 allowed us to avoid any zero field. For instance, addition of cylindrical permanent magnets with magnetization along the z-axis would have been less challenging, but such permanent magnets are characterized by an inversion of the direction of the magnetic field at the edges of the cylinder.

Our next aim is to broaden the applicability of our new method to other metabolic relevant molecules (e.g. pyruvate, urea, fumarate) and to start covering longer distances with the HP MCAs. By means of more advanced transportation devices, we plan to perform the hyperpolarization in our lab and run HP MRS animal experiments in a clinical environment.

Online Methods

Experimental design and implementation

Custom designed fluid path - CFP

The CFP was designed with the aim of being reusable, easily loading frozen solid samples and delivering to final users a "plug and play" closed device able to provide hyperpolarized injectable solutions with no need for a dDNP polarizer on site. The CFP is a combination of commercially available and custom-made components. Differently from the SPINlab version,[48] it does not present any glued joints between the parts in order to improve durability and limit failures during dissolution. Moreover, all plastic parts are made from polyether ether ketone (PEEK) or polyamide-imide (PAI). Refer to Figure 1 for the following description.

Figure 1A reports the device in its entirety. From top to bottom we find: (component 1) a stainless steel quick release (SS-QM2-B-200, Swagelok, Solon, OH, U.S.) that can be connected to a buffer boiler/dissolution head for dissolution or a He gas line for sample thermalization; (component 2) a modified PEEK plastic T-valve (P-713, IDEX Health & Science, Lake Forest, IL, U.S.); (component 3) a one-way valve (AKH04-00, SMC, Tokyo, Japan); (component 4) dynamic sealing; (component 5) top and (component 6) bottom part of a PEEK threaded vial.[32] Figure 1B, C and D show zoomed section views of the modified T-valve, dynamic sealing and threaded vial, respectively. A PAI conical transition (Figure B, component 7) connects the PEEK outer lumen (Figure 1C, component 8) and inner lumen (Figure 1C, component 9) inside the top arm of the T-valve and prevents any back flow towards the quick release. The T-valve's interior is modified to make a press fit between the inner lumen and the top arm of the T-valve while maximizing the flow in the bottom and right arms to split the gas/liquid inflow (orange arrow) from the outflow (cyan arrows). PEEK tubing is produced on demand (Zeus Inc., Orangeburg, NC, U.S.). The inner lumen (OD = 1.8 mm, ID = 1.6 mm) is extruded from natural PEEK (depicted in red in the figure to help distinguishing the different parts), while the outer lumen

(OD = 3.2 mm, ID = 2.4 mm) is extruded from PEEK containing a black pigment. The black pigment is necessary to laser weld the top part of the vial to the outer lumen (Figure 1D, component 11). The laser welding is performed by Leister Technologies (Kaegiswil, Switzerland). Compressing a PTFE O-ring (Figure 1D, component 12) between the top and bottom part of the threaded vial yields a leak rate < 10^{-8} mbar·L/s at room temperature. The integrity of the laser welding and PTFE O-ring sealing was also verified immersing the bottom part of the CFP in liquid nitrogen and pressurizing the device with He gas to 4 bar, without observing any pressure drop after 5 min. The inner lumen ends with a press fit PAI nozzle (Figure 1D, component 13) to improve dissolution performance. The dynamic sealing allows to load and unload the dDNP sample inside the polarizer while keeping it constantly at low pressure. Leak tightness as good as 10^{-8} mbar·L/s is achieved by compressing silicon O-rings (Figure 1D, components 10) around the outer lumen using purpose made threaded plugs. It is important to notice that the T-valve is passive. Therefore, to avoid cryo-pumping during sample loading and polarization, the one-way valve remains always connected to the right-arm of the T-valve. The dissolution capability and reliability of the CFP was tested in a series of 10 consecutive experiments. The vial was filled with 100 μL of a solution of blue colorant dissolved in glycerol:water 1:1 (v/v); the CFP was loaded inside the polarizer and let in superfluid He for 1 h; the dissolution was performed by heating 6 mL of phosphate buffer. No chase He case was used to blow out the sample. The dissolution was successful 10 times out of 10 with complete melting of the sample; the volume of HP solution collected inside a Falcon tube was 4.0 ± 0.5 mL. In a separate experiment the CFP was left inside the polarizer overnight and the next day dissolution was successful as well. See next section and ref. 37 for details about sample loading and dissolution procedure.

Magnetic enforced DNP probe

The second crucial hardware implementation dealt with a DNP probe that could shelter the sample hyperpolarization during extraction. Figure 6 shows drawings of the newly built DNP

probe: top part front view in Figure 6A, top part top view in Figure 6B, bottom part front view in Figure 6C, bottom part section view in Figure 6D, top part section view in Figure 6E. Refer to this figure for the following description.

Differently from Ji et al.,[27] we decided to equip the probe with NdFeB permanent magnets (Supermagnete, Gottmadingen, Germany) along the path travelled by the sample instead of winding the sample vial inside a small solenoidal electro-magnet to simplify extraction operations.

To cover with permanent magnets the full path's length experienced by the sample during extraction, we designed four different Halbach array arrangements. A four elements Halbach array (7.5 mm x 7.5 mm x 100 mm bar magnets), held in place by stainless steel squared profiles (Figure 6A, components 8), surrounds the probe stem (Figure 6C, components 12). The last four elements of this "magnetic rail" enter the top flange by 90% of its thickness (see Figure 6E, bottom inset). To fill the magnetic field gap between the ISO-KF-100 flange (Figure 6A, component 5) and the mini gate-valve (Figure 6A, component 3), four octagonal Halbach arrays (1.5 mm x 1.0 mm x 5 mm bar magnets) are stacked inside the two KF-16 half nipples (see Figure 6E, component 18). The mini gate-valve volume is covered by gluing on it a two elements Halbach array (30 mm x 30 mm x 10 mm block magnets) (see Figure 6E, right inset). A second stack of three octagonal Halbach arrays covers the gap between the mini gat-valve and loading chamber (Figure 6E, component 17). Finally, a 3D printed hexagonal Halbach array (12 mm x 12 mm x 12 mm block magnets) is placed around the bottom part of the loading chamber (Fig. 6 A, component 2) to insure sufficiently high magnetic field during transfer of the sample from the polarizer to the storage vessel. Details about the different Halbach arrays field profile are reported in Figure S5.

UV-sample preparation and handling

465 All chemicals were purchased from Sigma-Aldrich (Brøndby, Denmark) excepted for the radical
466 precursor deuterated trimethylpyruvic acid (d_9-TriPA) that was synthesized in house. We worked
467 with a single kind of sample whose preparation was optimized in a former publication.[30] [U-^{13}C,
468 d_7]-D-glucose was dissolved in 60±3 μL of glycerol:water 1:1 (v/v) to obtain a final glucose
469 concentration of 2.2M; d_9-TriPA was then added in amount corresponding to 10% of the final
470 volume; the solution was sonicated at 40°C for 5 min to efficiently degas the sample and improve
471 the glass quality after freezing. A solution volume of 6.0±0.3 μL was poured in liquid nitrogen as
472 a drop to form a frozen bead. The operation was repeated 10 times. The frozen sample was
473 transferred to a quartz Dewar (Magnettech, Berlin, Germany) filled with liquid nitrogen for UV
474 irradiation. The irradiation set up was extensively described earlier.[32] UV-light was shined on the
475 sample for 300 s using a broad-band source (Dymax BlueWave 75, Connecticut, U.S.) at full
476 power (i.e. 19 W/cm^2). Refer to Figure 7A for a simplified sketch of the setup. Radical
477 concentration was measured immediately after irradiation by inserting the tail of the quartz
478 Dewar in the cavity of an X-band spectrometer (Miniscope MS 5000, Magnettech, Berlin,
479 Germany) and following methods described earlier.[32] Finally, the irradiated frozen beads were
480 loaded inside the CFP vial bottom part (Figure 7B, component 4). While keeping it and the
481 bottom wrench (Figure 7B, component 5) in a Styrofoam box filled with liquid nitrogen, frozen
482 pellets were transferred, a new PTFE O-ring (Figure 7B, component 3) put in place and squeezed
483 by screwing the vial top part (Figure 7B, component 2) by means of the top wrench (Figure 7B,
484 component 1). A leak test was then performed pressurizing the CFP with helium gas (see ref. 32
485 and former section for details).

486 Sample loading inside the polarizer proceeded as follows. The polarizer variable temperature
487 insert (VTI) was kept filled with 10 cm of liquid He and at low pressure, the CFP was
488 disconnected from the leak-test station (see Figure S1) and the vial (Figure 1A, components 5
489 and 6) quickly displaced from the Styrofoam box filled with liquid nitrogen to the loading
490 chamber, while flushing the latter with He gas. The dynamic sealing (Figure 1A, component 4)

was lowered to close the loading chamber, the He gas flow shut down, and the gate-vale opened (Figure 6A, component 3). The vial was manually pushed to the center of the NMR coil (Figure 6D, component 15). The process took about 30 s in order to minimize liquid He evaporation (VTI pressure < 10 mbar). In its final position the vial touched the coil former (Figure 6D, component 16).

Microwave delivery and solid-state NMR measurements

Once the sample was in place, microwaves were delivered from a 94 GHz solid-state source VCOM-10/94-WPT (ELVA-1, St. Petersburg, Russia) coupled to a 200×2R4 frequency doubler (VDI, Charlottesville, VA, USA), which provided an output power of 55 mW at 188 GHz. The source, digitally controlled through NI-DAQ device USB-6525 (National Instruments, Austin, TX, U.S.) has a tuning range of ±0.6 GHz and the possibility to modulate the output frequency at a rate up to 2 kHz and with an amplitude of up to 100 MHz.

Microwaves reach the probe cavity (Figure 6C, component 13) travelling through a circular waveguide (Figure 6A, component 6) ending with a 45° mirror (Figure 6D, component 14) that reflects the microwaves towards the sample. In all experiments microwave irradiation was performed at optimal conditions: the output power was 55 mW and the frequency was modulated, following a sinusoidal profile, at a rate of 1kHz by 25 MHz around the central frequency 188.21 GHz. The latter corresponded to the negative maximum enhancement of the DNP spectrum.[30]

All ^{13}C NMR acquisitions were performed using a compact bench-top spectrometer (Kea2, Magritek, Wellington, New Zealand) connected to the DNP probe via a rigid coax-cable (Figure 6, component 7). Details about the NMR and microwave delivery performances were published earlier.[40,49] The flip angle used for all acquisitions was 1° (pulse length = 5 μs; transmitted power = 5 W). The polarization build-up was monitored by pulsing every 60 s. Relaxation after

thermalization was acquired by pulsing every 10 min. The thermal equilibrium signal build-up was monitored overnight pulsing every 30 min, after saturation of any residual signal with a 50'000 rf pulses comb. The NMR signal was acquired every 30 min (1 average) until complete relaxation was achieved. The DNP enhancement was calculated by dividing the thermal equilibrium and DNP signal integrals.

Dissolution and liquid-state NMR measurements

6 mL of 40 mM phosphate buffer containing 0.1 g/L of Ethylenediaminetetraacetic acid (EDTA) was loaded into the CFP dissolution head/boiler (see Fig. S7) and pressurized to 4 bar with helium gas. The solution was heated to approx. 180 °C (12 bar of vapor pressure). For dissolutions from the polarizer, the VTI was kept at approx. 1 mbar, the CFP was lifted 15 cm out of the liquid helium, by sliding the outer lumen inside the dynamic sealing, and connected to an exit tube. The CFP inlet was then connected to the dissolution head, the hot buffer released, and the HP solution flushed out from the polarizer until the pressure in the dissolution head dropped to zero. The HP solution was recovered in a Falcon tube and manually injected into a 5 mm NMR tube. The superheated buffer reached the sample flowing through the CFP inner lumen. The melted sample came out from the polarizer flowing in between CFP inner and outer lumen. It finally flew through the one-way valve and reached the Falcon tube. When dissolving from the transportation device, all steps were as above, but the sample vial was not moved from the 1T storage magnet and the dissolution happened while keeping the vial in liquid nitrogen.

All dissolved HP samples were transferred to a 9.4 T Varian (Palo Alto, California, U.S.) vertical high-resolution spectrometer for measurements. The decay of the ^{13}C HP signal was monitored every 3 s with 5° pulses. Once complete relaxation was achieved the liquid sample in the NMR tube was doped with 10 µL of Dotarem® and reinserted into the spectrometer. The same 5° pulse was used to measure the signal corresponding to thermal equilibrium from 1024 averages with

100 ms repetition time. The DNP enhancement was obtained computing the ratio between the value of the integral of the first spectrum of the HP decay and the thermal equilibrium one.

Relaxation at longer term storage conditions

In a separate set of experiments, we measured the relaxion of a thermalized sample at 1 T and 4.2 K. To do so, we filled the polarizer with liquid He to a height of approximately 50 cm above the NMR coil and implemented a manual field cycling. A magnetic field of approx. 1 T corresponded to a vertical position of 25 cm above the isocenter of the polarizer (relaxation position). The field cycling happened as follows: the first data point was acquired after thermalization; the sample was then lifted to relaxation position and left there for 1 h; the sample was moved back inside the NMR coil to acquire the second data point. The procedure was repeated 5 times for a total duration of the experiment of 5 h.

Other instruments, simulations and data analysis

The leak detector used in this study was a Phoenix from Leybold GmbH (Cologne, Germany). The Hall probe device was a Lake Shore 475 from Lake Shore Cryotronics (Westerville, OH, U.S.) equipped with a longitudinal and axial probe to measure the magnetic field from the superconductor and Halbach arrays, respectively. All NMR data were processed in MNOVA (Mestrelab Research, Santiago de Compostela, Spain). Magnetic field simulations were performed using MATLAB (Mathworks, Natick, MA, U.S.) and COMSOL 5.4 (COMSOL Multiphysics, Burlington, Massachusetts, U.S.). ESR data were processed in MATLAB. All plots were generated using Origin 2019 (OriginLab Corporation, Northampton, Massachusetts, U.S.)

Statistical analysis

All numerical results are reported in the main text as average of repeated measurements, and the standard deviation represents the error. All measurements were repeated at least three times

Acknowledgments

We thank Prof. Jean-Noël Hyacinthe for useful discussion and Dr Sebastian Meier for setting up "remote dissolution" experiments at the Chemistry Department. This work was supported by the Danish National Research Foundation (DNRF124); the European Union's Horizon 2020 research and innovation programme under the Marie Sklodowska-Curie grant agreement no. 713683 (COFUNDfellowsDTU); and the Swiss National Fund under the SPARK grant agreement no. CRSK-2_190547 and Ambizione grant agreement no. PZ00P2_193276.

Author contributions

Capozzi, Kilund, Lerche and Ardenkjær-Larsen study conception and design. Capozzi, Kilund, Karlsson, Pinon, Patel, Lerche acquisition of data. Capozzi, Karlsson, and Lerche analysis and interpretation of data. Ouari and Patel synthesis of non-persistent radical precursor. Capozzi and Lerche drafting of manuscript. Ouari, Ardenkjær-Larsen and Karlsson critical revision.

Competing financial interests

Prof. Ardenkjær-Larsen is CEO of the startup company Polarize. Polarize sells dDNP equipment for pre-clinical studies

Additional information

The supplementary material listed below is available for this paper online.

Figure S1. Leak-test station.

Figure S2. Radical leftover after quenching procedure.

Figure S3. Sample relaxation after thermalization at 4.2 K and 1 T.

Figure S4. Measurements and simulation of the polarizer stray magnetic field.

Figure S5. Finite elements simulations of the different Halbach arrays placed inside the new DNP probe. Part1.

Figure S6. Finite elements simulations of the different Halbach arrays placed inside the new DNP probe. Part2.

Figure S7. Finite element simulation for storage magnet.

Figure S8. Compact dissolution station head.

Movie S1. Hyperpolarization transport at storage conditions of 77 K and 1 T

 Correspondence and requests for materials should be addressed to email: andrea.capozzi@epfl.ch. Raw data are available upon request.

References

1. van de Weijer, T. & Schrauwen-Hinderling, V. B. Application of Magnetic Resonance Spectroscopy in metabolic research. *Biochim. Biophys. Acta BBA - Mol. Basis Dis.* **1865**, 741–748 (2019).
2. Haris, M. *et al.* Molecular magnetic resonance imaging in cancer. *J. Transl. Med.* **13**, 313 (2015).
3. Zilberter, Y. & Zilberter, M. The vicious circle of hypometabolism in neurodegenerative diseases: Ways and mechanisms of metabolic correction: Hypometabolism in Neurodegenerative Diseases. *J. Neurosci. Res.* **95**, 2217–2235 (2017).
4. Fuss, T. L. & Cheng, L. L. Metabolic Imaging in Humans. *Top. Magn. Reson. Imaging* **25**, 223–235 (2016).
5. Bonvento, G., Valette, J., Flament, J., Mochel, F. & Brouillet, E. Imaging and spectroscopic approaches to probe brain energy metabolism dysregulation in neurodegenerative diseases. *J. Cereb. Blood Flow Metab.* **37**, 1927–1943 (2017).
6. Kelloff, G. J. *et al.* Progress and Promise of FDG-PET Imaging for Cancer Patient Management and Oncologic Drug Development. *Clin. Cancer Res.* **11**, 2785–2808 (2005).
7. Shreve, P. D., Anzai, Y. & Wahl, R. L. Pitfalls in Oncologic Diagnosis with FDG PET Imaging: Physiologic and Benign Variants. *RadioGraphics* **19**, 61–77 (1999).
8. Long, N. M. & Smith, C. S. Causes and imaging features of false positives and false negatives on 18F-PET/CT in oncologic imaging. *Insights Imaging* **2**, 679–698 (2011).
9. Brender, J. R. *et al.* Dynamic Imaging of Glucose and Lactate Metabolism by 13C-MRS without Hyperpolarization. *Sci. Rep.* **9**, 3410 (2019).

10. Gutte, H. *et al.* Simultaneous hyperpolarized (13)C-pyruvate MRI and (18)F-FDG-PET in cancer (hyperPET): feasibility of a new imaging concept using a clinical PET/MRI scanner. *Am. J. Nucl. Med. Mol. Imaging* **5**, 38–45 (2015).
11. Gialleonardo, V. D., Wilson, D. M. & Keshari, K. R. The Potential of Metabolic Imaging. *Semin. Nucl. Med.* **46**, 28–39 (2016).
12. De Feyter, H. M. *et al.* Deuterium metabolic imaging (DMI) for MRI-based 3D mapping of metabolism in vivo. *Sci. Adv.* **4**, eaat7314 (2018).
13. Wang, Z. J. *et al.* Hyperpolarized ^{13} C MRI: State of the Art and Future Directions. *Radiology* **291**, 273–284 (2019).
14. de Graaf, R. A., Rothman, D. L. & Behar, K. L. State of the art direct 13C and indirect 1H-[13C] NMR spectroscopy in vivo. A practical guide: A PRACTICAL GUIDE TO 13C AND 1H-[13C] NMR IN VIVO. *NMR Biomed.* **24**, 958–972 (2011).
15. Nelson, S. J. *et al.* Metabolic Imaging of Patients with Prostate Cancer Using Hyperpolarized [1-$^{13\$}$C]Pyruvate. *Sci. Transl. Med.* **5**, 198ra108 1–10 (Aug 14).
16. Grist, J. T. *et al.* Quantifying normal human brain metabolism using hyperpolarized [1–13C]pyruvate and magnetic resonance imaging. *NeuroImage* **189**, 171–179 (2019).
17. Ardenkjaer-Larsen, J. H. *et al.* Increase in signal-to-noise ratio of > 10,000 times in liquid-state NMR. *Proc. Natl. Acad. Sci. U. S. A.* **100**, 10158–10163 (Sep 2).
18. Golman, K. & Petersson, J. S. Metabolic imaging and other applications of hyperpolarized C-13. *Acad. Radiol.* **13**, 932–942 (2006).
19. Kurhanewicz, J. *et al.* Hyperpolarized (13)C MRI: Path to Clinical Translation in Oncology. *Neoplasia* **21**, 1–16 (2019).

20. Chen, H.-Y. *et al.* Hyperpolarized 13C-pyruvate MRI detects real-time metabolic flux in prostate cancer metastases to bone and liver: a clinical feasibility study. *Prostate Cancer Prostatic Dis.* (2019) doi:10.1038/s41391-019-0180-z.

21. Gallagher, F. A. *et al.* Imaging breast cancer using hyperpolarized carbon-13 MRI. *Proc. Natl. Acad. Sci.* **117**, 2092–2098 (2020).

22. Peat, D. T. *et al.* Low-field thermal mixing in [1- ^{13}C] pyruvic acid for brute-force hyperpolarization. *Phys. Chem. Chem. Phys.* **18**, 19173–19182 (2016).

23. Wolber, J. *et al.* Generating highly polarized nuclear spins in solution using dynamic nuclear polarization. *Nucl. Instrum. Methods Phys. Res. Sect. Accel. Spectrometers Detect. Assoc. Equip.* **526**, 173–181 (2004).

24. Abragam, A. & Goldman, M. Principles of Dynamic Nuclear-Polarization. *Rep. Prog. Phys.* **41**, 395–467 (1978).

25. Blumberg, W. E. Nuclear Spin-Lattice Relaxation Caused by Paramagnetic Impurities. *Phys. Rev.* **119**, 79–84 (1960).

26. Hirsch, M. L., Kalechofsky, N., Belzer, A., Rosay, M. & Kempf, J. G. Brute-Force Hyperpolarization for NMR and MRI. *J. Am. Chem. Soc.* **137**, 8428–8434 (2015).

27. Ji, X. *et al.* Transportable hyperpolarized metabolites. *Nat. Commun.* **8**, (2017).

28. Capozzi, A., Cheng, T., Boero, G., Roussel, C. & Comment, A. Thermal annihilation of photo-induced radicals following dynamic nuclear polarization to produce transportable frozen hyperpolarized 13C-substrates. *Nat. Commun.* **8**, 15757 (2017).

29. Bornet, A. *et al.* Boosting Dissolution Dynamic Nuclear Polarization by Cross Polarization. *J. Phys. Chem. Lett.* **4**, 111–114 (Jan 3).

30. Capozzi, A. *et al.* Efficient Hyperpolarization of U-(13) C-Glucose Using Narrow-Line UV-Generated Labile Free Radicals. *Angew Chem Int Ed Engl* **58**, 1334–1339 (2019).

31. Eichhorn, T. R. *et al.* Hyperpolarization without persistent radicals for in vivo real-time metabolic imaging. *Proc. Natl. Acad. Sci. U. S. A.* **110**, 18064–18069 (Nov 5).

32. Capozzi, A., Karlsson, M., Petersen, J. R., Lerche, M. H. & Ardenkjaer-Larsen, J. H. Liquid-State ^{13}C Polarization of 30% through Photoinduced Nonpersistent Radicals. *J. Phys. Chem. C* **122**, 7432–7443 (2018).

33. Patel, S. *et al.* UV-Irradiated 2-Keto-(1-^{13}C)Isocaproic Acid for High-Performance ^{13}C Hyperpolarized MR. *J. Phys. Chem. C* **124**, 23859–23866 (2020).

34. Mishkovsky, M. *et al.* Measuring glucose cerebral metabolism in the healthy mouse using hyperpolarized C-13 magnetic resonance. *Sci. Rep.* **7**, (2017).

35. Rodrigues, T. B. *et al.* Magnetic resonance imaging of tumor glycolysis using hyperpolarized C-13-labeled glucose. *Nat. Med.* **20**, 93-+ (2014).

36. Meier, S., Karlsson, M., Jensen, P. R., Lerche, M. H. & Duus, J. O. Metabolic pathway visualization in living yeast by DNP-NMR. *Mol. Biosyst.* **7**, 2834–2836 (2011).

37. Pinon, A. C., Capozzi, A. & Ardenkjær-Larsen, J. H. Hyperpolarized water through dissolution dynamic nuclear polarization with UV-generated radicals. *Commun. Chem.* **3**, 57 (2020).

38. Malinowski, R. M., Lipso, K. W., Lerche, M. H. & Ardenkaer-Larsen, J. H. Dissolution Dynamic Nuclear Polarization capability study with fluid path. *J. Magn. Reson.* **272**, 141–146 (2016).

39. Lipso, K. W., Bowen, S., Rybalko, O. & Ardenkjaer-Larsen, J. H. Large dose hyperpolarized water with dissolution-DNP at high magnetic field. *J Magn Reson* **274**, 65–72 (2017).

40. Albannay, M. M., Vinther, J. M. O., Capozzi, A., Zhurbenko, V. & Ardenkjaer-Larsen, J. H. Optimized microwave delivery in dDNP. *J. Magn. Reson.* **305**, 58–65 (2019).

41. Capozzi, A. *et al.* Gadolinium Effect at High-Magnetic-Field DNP: 70% ^{13}C Polarization of [U-^{13}C] Glucose Using Trityl. *J. Phys. Chem. Lett.* **10**, 3420–3425 (2019).

42. Radaelli, A. *et al.* ^{13}C Dynamic Nuclear Polarization using SA-BDPA at 6.7 T and 1.1 K: Coexistence of Pure Thermal Mixing and Well-Resolved Solid Effect. *J. Phys. Chem. Lett.* **11**, 6873–6879 (2020).

43. Hirsch, M. L. *et al.* Transport and imaging of brute-force 13 C hyperpolarization. *J. Magn. Reson.* **261**, 87–94 (2015).

44. Latanowicz, L. NMR relaxation study of methyl groups in solids from low to high temperatures. *Concepts Magn. Reson. Part A* **27A**, 38–53 (2005).

45. Guarin, D. *et al.* Characterizing Thermal Mixing Dynamic Nuclear Polarization via Cross-Talk between Spin Reservoirs. *J. Phys. Chem. Lett.* **8**, 5531–5536 (2017).

46. de Boer, W., Borghini, M., Morimoto, K., Niinikoski, T. O. & Udo, F. Dynamic polarization of protons, deuterons, and carbon-13 nuclei: Thermal contact between nuclear spins and an electron spin-spin interaction reservoir. *J. Low Temp. Phys.* **15**, 249–267 (1974).

47. Borghini, M. Spin-Temperature Model of Nuclear Dynamic Polarization Using Free Radicals. *Phys. Rev. Lett.* **20**, 419- (1968).

48. Ardenkjaer-Larsen, J.-H. *et al.* Dynamic nuclear polarization polarizer for sterile use intent. *NMR Biomed.* **24**, 927–932 (2011).

49. Albannay, M. M., Vinther, J. M. O., Petersen, J. R., Zhurbenko, V. & Ardenkjaer-Larsen, J. H. Compact, low-cost NMR spectrometer and probe for dissolution DNP. *J. Magn. Reson.* **304**, 7–15 (2019).

Figures

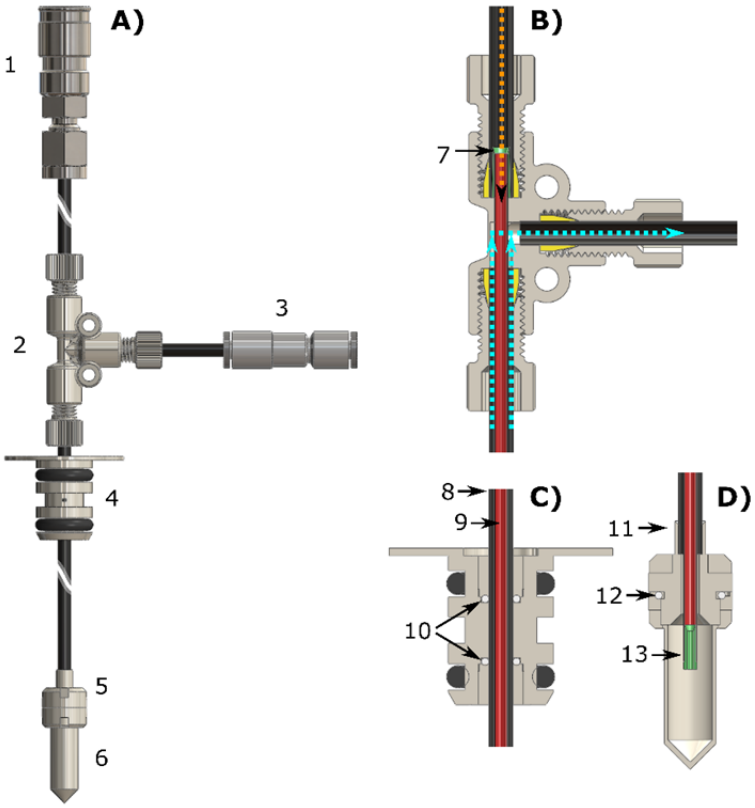

Fig. 1. Custom fluid path (CFP) illustration. Technical drawings of the CFP (**A**) and zoomed section of the T-valve indicating inner (orange arrow) and outer (cyan arrows) flow directions (**B**), dynamic sealing (**C**) and sample threaded vial (**D**). Numbers indicates the most important components of the device: quick release connection (1), T-valve (2), one-way valve (3), dynamic sealing (4), vial top part (5), vial bottom part (6), outer-lumen to inner-lumen transition (7), black PEEK outer-lumen (8), red PEEK inner-lumen (9), dynamic sealing silicon O-ring (10), laser welded joint (11), vial PTFE O-ring (12), nozzle (13).

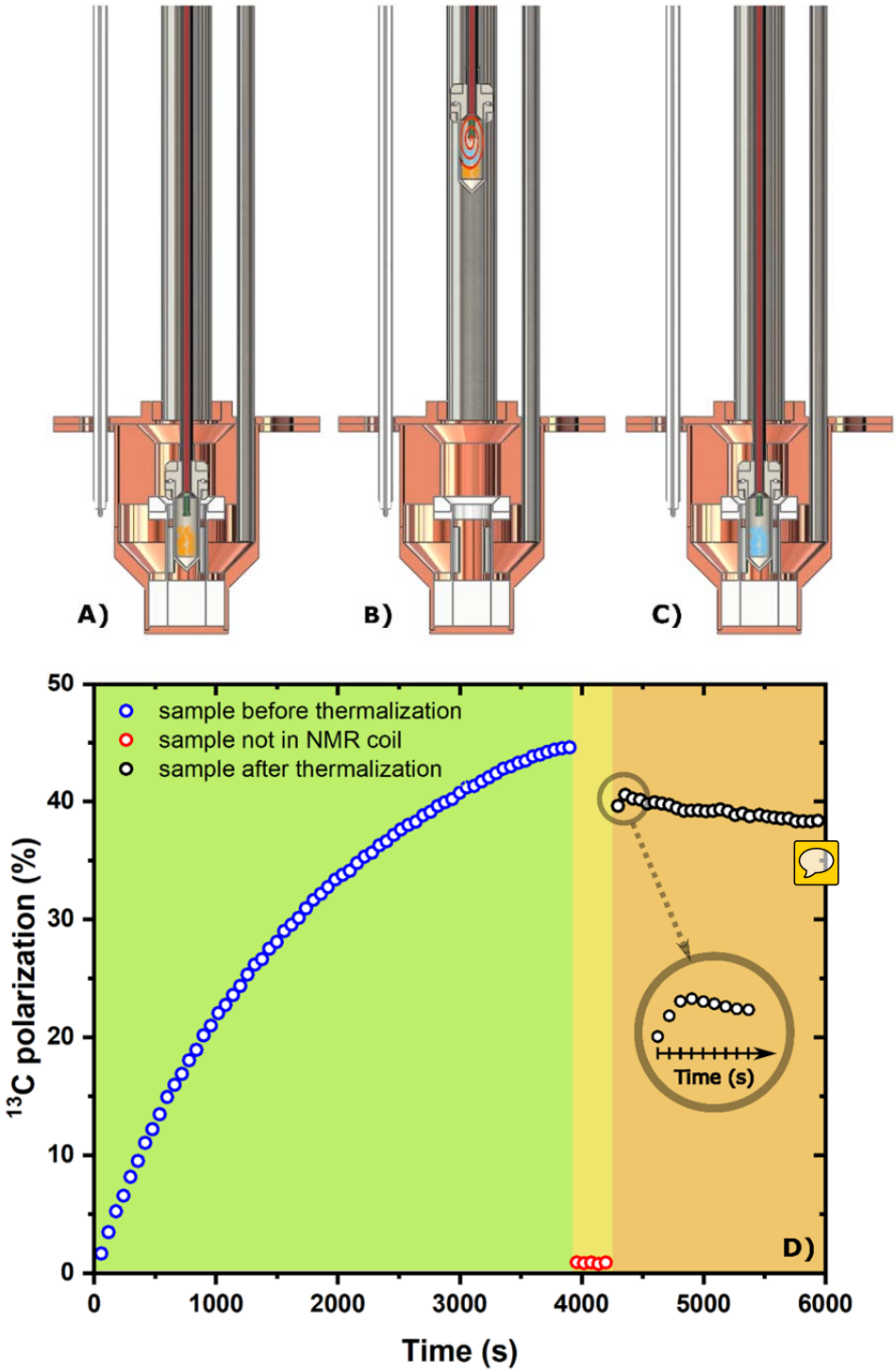

Figure 2. Different steps of a radicals scavenging experiment at 6.7 T and 1.2 K. First, the sample sits inside the NMR coil and it is fully polarized. (**A**). A mono-exponential fit to the data provided a build-up time constant of 1300 ± 10 s (R2 = 0.99, not shown). Second, the sample vial

is lifted by 15 cm above the liquid He level and left there for 5 min; the CFP inlet is connected to a He gas line; room temperature He gas is blown on the frozen beads (**B**). Finally, after thermalization of the sample, the vial is lowered back inside the NMR coil for measurements (**C**). Yellow pellets represent sample beads before radical removal, while blue pellets represent sample beads after the thermalization process. The orange spiral represents the He gas flow inside the vial during thermalization. The NMR signal corresponding to panel (**A**), (**B**) and (**C**) is reported in panel (**D**) in the green, yellow and orange portion of the graph respectively; each data point was acquired every 60 s. The inset is a magnification of the first 90 s just after the sample goes back to measurement position. Each point was acquired every 10 s.

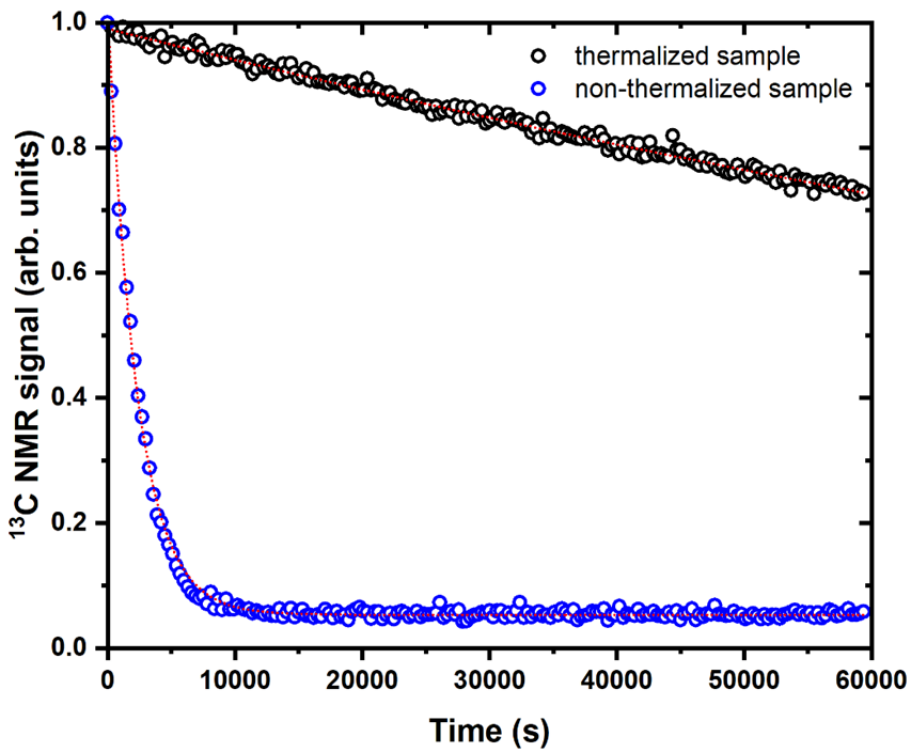

Figure 3. ended spin-lattice relaxation for a sample after quenching of the radicals at 6.7 T and 4.2 K. ^{13}C T_1 measurements for a thermalized (black circles) and non-thermalized sample (blue circles). Each experimental data point was acquired every 10 min. Red dotted curves are the

result of a mono-exponential fit to the data. The T_1 values for the non-thermalized and thermalize sample were 2300 ±20 s and 200000±3600 s, respectively (R^2 = 0.99).

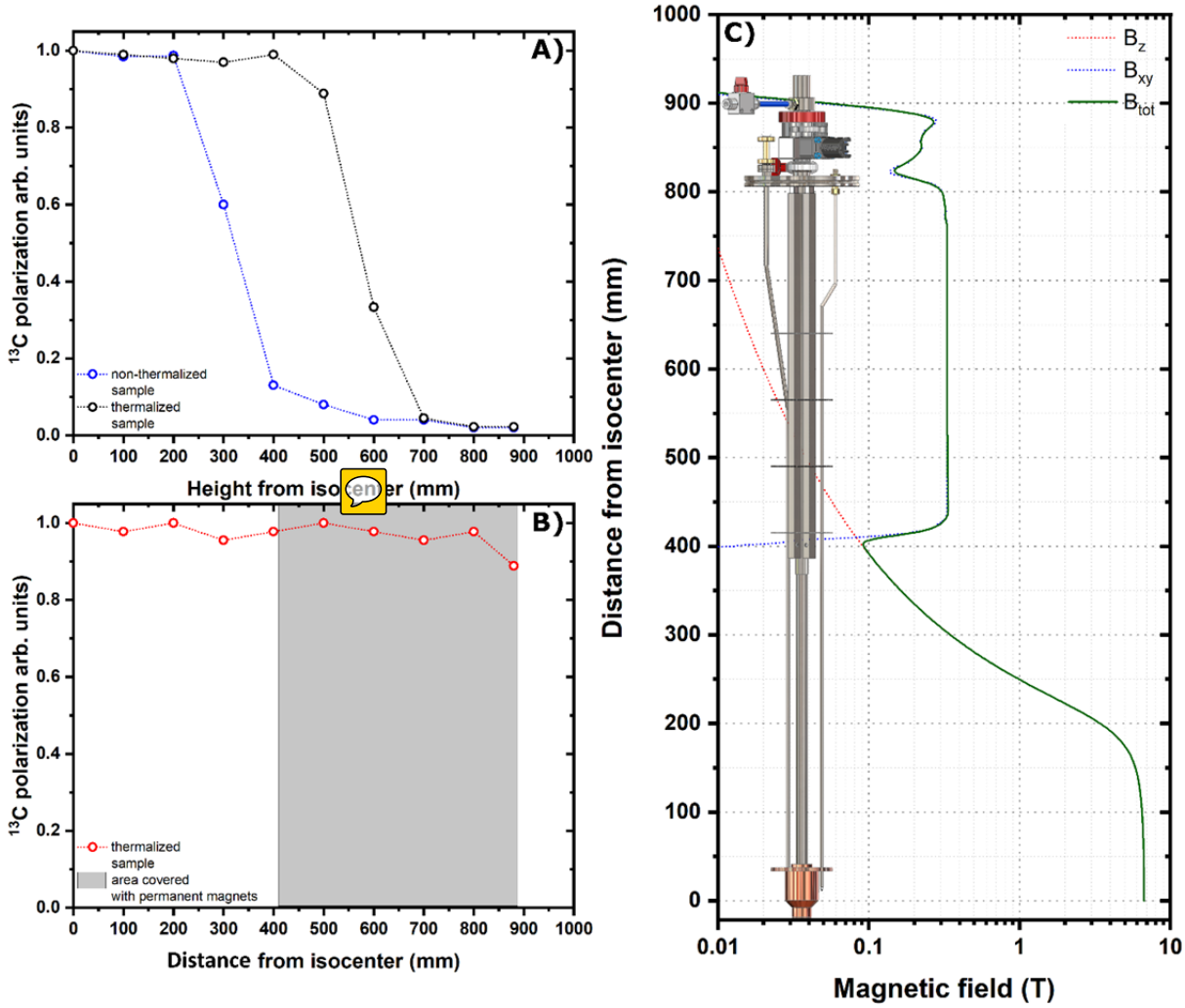

Figure 4. Sample extraction and hyperpolarization sheltering method. ^{13}C polarization losses as a function of the sample vertical position inside the polarizer while using a traditional DNP probe. The experiment was repeated for a non-thermalized sample (blue circles) and a thermalized sample (black circles) (**A**). ^{13}C polarization losses as a function of the sample vertical position inside the polarizer while using our new DNP probe equipped with permanent magnets. The experiment was performed for a thermalized sample only (red circles). The gray shaded area

represents the area covered by permanent magnets in the new probe. The last point was measured after lifting the sample up to the loading chamber and closing the mini-gate valve for 10 s (**B**). Calculated magnetic field value as a function of the distance from the polarizer isocenter. The magnetic field generated by the polarizer coil is parallel to the probe axis (red dotted line), while the magnetic field generated by the permanent magnets is perpendicular to the probe axis (blue dotted line). The norm of the total field is also reported (green continuous line) (**C**).

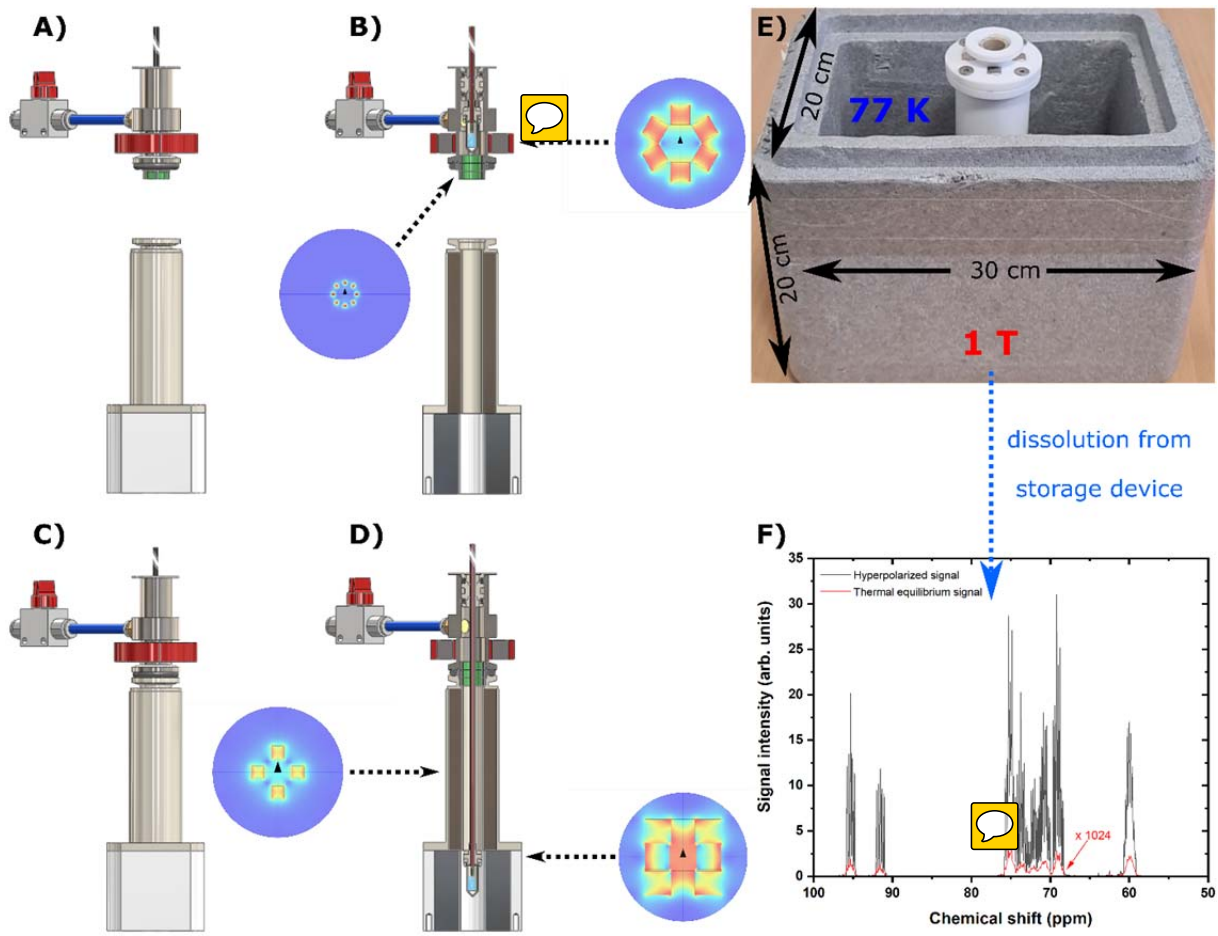

Figure 5. HP solid transport and remote dissolution. We report here a schematic of our strategy for storage/transport of a HP sample and remote dissolution. After lifting up the sample vial above the gate valve, the transport procedure entails 4 main steps. First, the loading chamber/air lock is disconnected from the polarizer and docked to the transport device (**A**) and

(**B**). Second, the sample vial is pushed down to reach the 1 T magnet (**C**) and (**D**). The transport device is composed by two parts: a four elements 300 mT Halbach array magnetic guide at the top and an eight elements 1 T Halbach array storage magnet at the bottom. The transportation device is placed inside a Styrofoam box and plunged in liquid nitrogen (**E**). Third, the Styrofoam box is transported to the site where the dissolution experiment is going to happen. Fourth, the CFP quick release is connected to the dissolution station (see Supporting Material) and the HP solution obtained and transferred to the NMR 9.4 T spectrometer for measurements (**F**).

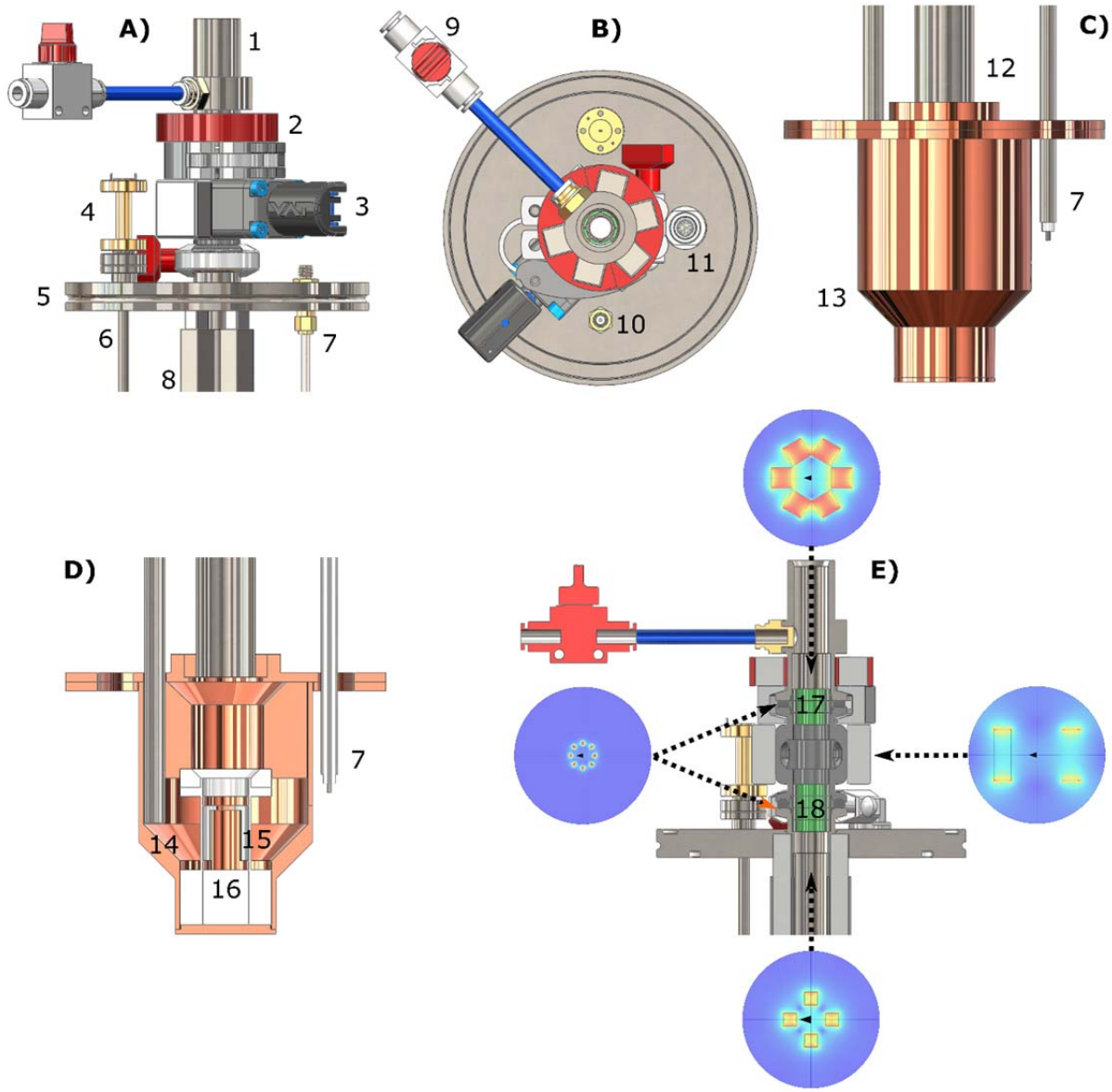

Figure 6. New DNP probe for sample extraction. Top and bottom part of the DNP probe are reported: top part front view (**A**), top part top view (**B**), bottom part front view (**C**), bottom part section view (**D**), top part front section view with simulated permanent magnets field profile cross section (**E**). Numbers indicates the main components: sample loading chamber (1), loading chamber hexagonal Halbach array placed around loading chamber (2), mini gate-valve with NdFeB permanent magnets (3), WR5-to-circular microwave transition (4), ISO-KF-100 flange (5), circular waveguide (6), NMR rigid coax-cable (7), squared Halbach array around probe stem/loading tube (8), loading chamber He gas purging line (9), NMR bulkhead SMA connector (10), Fischer connector for liquid helium level meter (11), probe stem (12), microwave cavity (13), 45° microwave mirror (14), pseudo Alderman-Grant coil (15), PTFE coil former (16), octagonal Halbach arrays inside KF16 flanges (17, 18).

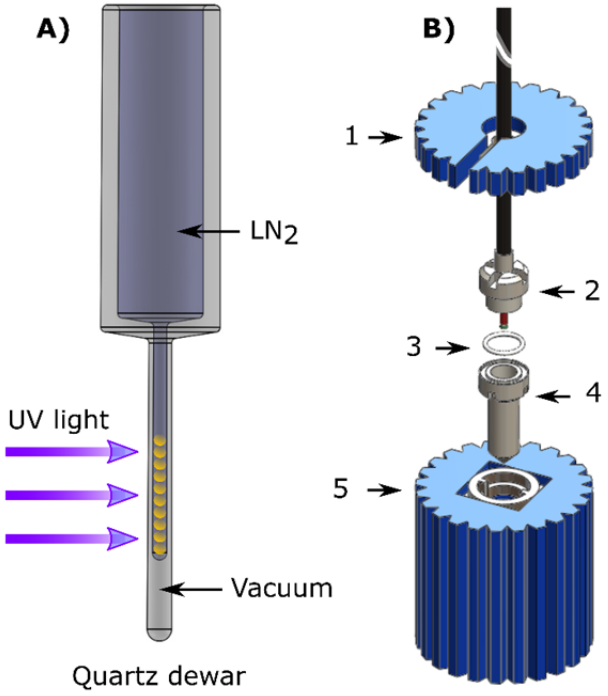

Figure 7. UV-irradiation and sample vial loading. The sample frozen beads are first UV-irradiated in liquid nitrogen (**A**). After irradiation and consequent radical generation, the sample

is ready for DNP (**B**): the bottom part of the sample vial (4) sits inside the bottom wrench (5) in liquid nitrogen; the irradiated sample is transferred into the vial, a new PTFE O-ring (3) put in place and squeezed by the top part of the vial (2) using the top wrench (1).

Reviewer #2 (Remarks to the Author):

In this work the authors nicely present a method to preserve the hyperpolarized state of metabolic contrast agents outside the polarization instrument. This is a major achievement that may lift a major barrier in metabolic hyperpolarized magnetic resonance research and allow other players to enter the field. The authors nicely discuss the achievements and the problems still to solve.
The technology is demonstrated on [U-13C, d7]-D-glucose, an agent with a relatively short lifetime compared to the main dDNP agent [1-13C]pyruvate and therefore more challenging.

I have reviewed the parts within my expertise. I am not an expert on magnetic field simulations or hardware design, including the design of NMR probes or permanent magnets. I would trust the authors on those due to their track record in designing and implementing such instrumentation and the level of detail given.

I only have minor comments as regards to the text.

Introduction

1. "characterized by high glucose uptake" is not clear in the context of this statement.

We have modified the sentence which now reads: "and in inflamed normal tissue with the risk of false positives".

2. As regards to FDG-PET, please indicate more clearly the ionizing radiation to which patients are exposed to and the limitations on repeated examinations and use in certain patient populations.

We have removed a sentence and two references to put less emphasis on PET-FDG which is in any case not a target of investigation in this paper. We modified another sentence. The relevant sentence now reads:" The use of ^{18}F-FDG PET agents exposes the patient to gamma-rays, which restricts its use (e.g. in certain patient groups and for repeated examinations)."

3. "good spectral separation" – not clear

We have modified the sentence which now reads: "These techniques allow characterization of tumors by measuring downstream metabolism enabled by difficult signal disentanglement of the different metabolites"

4. The authors place major focus on the comparability to FDG-PET operational considerations. In this regard:
a. FDG-PET uses a 2-deoxyglucose derivative, please indicate that the parallel agent to this in hyperpolarized MR

would be a stable isotope labeled 2-deoxyglucose agent. Please cite DOI: 10.1038/s41598-019-56063-0 in this regard.

We agree with the reviewer that there has been put too much emphasis on the comparability to FDG-PET. We have modified both the abstract and also the introduction to reflect that this paper is not infact a study that concerns such comparison. Accordingly, we will not include the suggested paper since it is no longer relevant.

b. The first use of hyperpolarized [U-13C, d7]-D-glucose for MR imaging that parallels the FDG-PET examination (without metabolic pathway resolution) was reported several years ago and should be cited, DOI: 10.1002/cmmi.1497.

We have included this reference (now ref. 36) along with the other cited references concerning [U-13C, d7]-D-glucose.

Results

5. The section "A "make it all" device" is not results. I would move this to the Methods in a separate section on the Description of the system. The same goes for the 1st paragraph of the section "Hyperpolarized sample with extended lifetime". The same goes for Figure 1 and Figure 6.

We agree with the reviewer that "a make it all device" sounds like a method section and it is somewhat redundant with "Custom designed fluid path" paragraph in the method. Nevertheless, this was a key development for this project. Therefore, we would like to keep Fig. 1 where among the results to give emphasis to this tool, but we rewrote the concerned paragraph keeping it short and limited to results only. We also changed the heading to "CFP performance" to be compliant to comment of reviewer 2. The heading "Hyperpolarized sample with extended lifetime" was also eliminated and the corresponding paragraph was included in "CFP performance". Differently Figure 6 is already part of the methods. Because of the format of the journal (Methods after Results), in the "CFP performance" paragraph we kept only the fundamental "Methods information" to facilitate the reader understanding (e.g. sample composition and DNP working conditions). The new paragraph writes:

"CFP performance

The CFP (see Figure 1, all technical details are reported in *Methods*) allowed us to investigate, in a robust and reproducible way, all steps involved in a "remote DNP" experiment employing UV-induced radicals: UV-irradiated sample loading into the dDNP polarizer while keeping it below the critical temperature of around 190 K, hyperpolarization of the sample, UV-radicals elimination, HP sample extraction from the polarizer, HP sample storage and transport and finally HP sample dissolution away from the production site.

After 5 min of UV-light irradiation 40±4 mM (n = 3) of radical was generated into the solid sample (see *Methods* for details about sample preparation). During sample loading into the polarizer the pressure increased from the base

pressure of 1 mbar to 10 mbar and went back to the initial value within 1 min. Performing DNP at 6.7 T/1.20±0.05 K under optimal microwave irradiation, ^{13}C nuclei could reach a solid-state polarization of 45±5 % with a buildup time constant 1300 ±10 s (n = 3), in good agreement with our former study.[30] The polarization step of the experiment is sketched in Figure 2A, and a typical DNP buildup curve of the sample is reported in the green portion of Figure 2D.

The quenching step is sketched in Figure 2B. Before blowing He gas onto the sample for 20 s at 6 bar of pressure, best results were obtained by first switching OFF the microwaves, then lifting the vial 15 cm above the NMR coil, outside the liquid He bath, and leaving it there for 5 min (see absence of recorded NMR signal in the yellow portion of Figure 2D).The different parameters (i.e. blowing time, blowing pressure, quenching position and waiting time) of the procedure were optimized in repeated experiments. This allowed us to get rid of 99% of the radical in the sample (see Figure S2), while measuring a polarization loss of 20% of the initial polarization values (see orange portion of Figure 2D), when reinserting the vial into the NMR coil (see Figure 2C). The inset in Figure 2D shows the "signature" of a successful thermalization experiment: the signal increased in the first few recorded NMR spectra.

Quenching of most of the radicals was confirmed by the absence of any DNP process when switching the microwaves back ON, and it caused a dramatic increase of ^{13}C nuclear spin-lattice relaxation time. The latter, measured at 4.2 K and 6.7 T, increased from 2,300 ±20 s for a non-quenched sample to 200,000±3,600 s (i.e. 55±1 h) for a quenched sample (see Figure 3), confirming that the UV-radicals represented the main source of relaxation.

In a separate series of experiments, by implementing a manual field cycling inside the polarizer, we also measured the ^{13}C relaxation of a sample after UV-radicals quenching at 4.2 K and 1 T (see *Methods* for details about the field cycling implementation). In Figure S3 we report the results: by fitting a mono-exponential curve to data, we found a T_1 of 4.0±0.5 h (R^2 = 0.97)."

6. Movie S1 is important and well presented, maybe I missed it but how long did the transfer procedure take here actually? From the rest of the text (Discussion) it is not clear if the time to reach the dissolution site was 3 min or the dissolution procedure took 3 min from arrival to the dissolution site. I thought the latter as per the description in the Results but the paragraph starting with "A more potent source…" in the discussion confused me.

Yes, it was the time it took to go from the polarizer to the dissolution site. The dissolution procedure and transfer of the HP solution took 10 s as usual.

Discussion

7. What would be the role of the [U-13C, d7]-D-glucose formulation? The authors understandably use a formulation already used by this group. However, it should be noted that other formulations have been developed

and studied for this agent (even if in a different magnetic field). For example, please see DOI: 10.1002/cphc.201900946.

We chose this formulation for the high achievable polarization that glucose can reach when using UV-induced radicals. The work suggested by the reviewer, although of relevance at the more common field of 3.35 T, it concerns the trityl radical together with Gd doping. Trityl is a permanent radical and this kind of samples cannot the transported. Therefore, we will not include the suggested reference

8. Sentence starting with "Under these conditions, the T1 measured…" unclear.

We specified the concerned sentence by indicating clearly the value of T1 we estimate (i.e. 5 min at 77 K and 1 T).

Online methods

9. Dissolution: It is not clear why one would dissolve a glucose sample in a phosphate buffer as glucose is not acidic. The dissolution buffer appears hypo-osmotic and contains EDTA, both are likely to lead to prolonged T1 compared to solutions intended for biological use.

While we agree with the reviewer that the buffer used in the glucose demonstration is not going to be the choice in a clinical injectable, in particular since, as the reviewer points out, the injectable needs to be isotonic. In the present study, however, the demonstration did not hold such limitation and we chose to use a standard buffer for our ^{13}C MCA studies where EDTA is added to prevent metal ions released in the heated boiler to impact the T_1 negatively. The phosphate buffer has no impact on glucose T1.

10. Enhancement calculation: 100 ms repetition time seems really short for 13C of glucose. Was this time enough for obtaining fully relaxed spectra? If not, is the T1 under these conditions known? Was the line-width affected by Gd doping? Could it be that this affected the polarization % that was determined?

We did not observe any substantial broadening from Gd doping on ^{13}C; actually TR is 1.1 s (1s of FID acquisition + 0.1 s delay). Taking into account a measured T1 of glucose in presence of Gd (Omniscan) of 0.4 s and a flip angle of 5 deg, the error on the thermal equilibrium signal is below 1%. We updated in methods the TR to be 1.1 s.

11. Page 22: relaxion, correct

OK

Reviewer #3 (Remarks to the Author):

The authors report a very important improvement to dDNP: the transfer of frozen samples with long T1. The present some modification to a DNP system that allows them to keep the sample at an elevated magnetic field to reduce relaxation losses. the sample is transfered to an NMR and detected. A few % polarization were observed on glucose.

This report is an essential progress that must be published.

Unfortunately, I have some issues with the scholary presentation of the work. I find many superfluous sentences, colloquialisms, unclear structures on the one hand, and litte substantial data on the other (eg. on chemistry, its a chemistry journal after all). The abstract (which is not an abstract in my opinion) is even a bit missleading in suggesting that you solved the T1 issue of glucose. The short T1 in vivo remains the major issue which is not addressed at all (see paper by Rodrigues et al). You dont explicitly say that you did, but you don't deny either, and in the context is appears as such.

We have modified the abstract to a concise presentation of motivation and the findings of the paper:

"Hyperpolarized (HP) ^{13}C-labelled metabolic contrast agents (MCAs) via dissolution Dynamic Nuclear Polarization (dDNP) can, non-invasively and in real-time, report on tissue specific aberrant metabolism. However, a short signal lifetime of these agents combined with the need to invest in demanding and expensive hyperpolarization equipment hamper the adoption of the method in the clinic.

In this work, we provide a robust methodology that allow remote production of the hyperpolarized ^{13}C-MCA. The methodology, built on photo-induced thermally labile radicals, allows solid sample extraction from the dDNP polarizer and hours long lifetime of the ^{13}C-MCAs at appropriate experimental conditions. We demonstrate the ability to disconnect the elaborate HP equipment from its end-user site. Exemplified with [U-^{13}C, d_7]-D-glucose, we remotely produce above 10,000-fold signal enhancement on the ^{13}C-MCA at 9.4 T, enabled by HP sample storage, transport and on-site dissolution."

You will find many comments in the attached file, unclear language is highlighted.
Thus I strongly encourage the authors to revise this utterly important paper make to make it more matter-of-fact-style, to tone down many expessions and to give realistic assessement of Glucose. To be honest, I don't see Glucose going anywhere until T1 in vivo is longer, so it may not be the perfect molecule to demonstrate delivery of HP samples, but as a demonstrator its OK.

We agree that glucose as well as most other hyperpolarized molecules are challenged by a short T_1 *in vivo* and that this paper only addresses the path from production to injection of the MCA. We have modified the text to make this point very clear.

We do however believe that the point made by the reviewer not only applies to glucose but is a general issue for the hyperpolarization technique. Rodrigues et al. reports an apparent in vivo T1 of 9s. This value is similar to the apparent in vivo T1 of pyruvate (approx. 12 s) at the same field strength and in mice. While pyruvate has a short T1 already in blood due to unfavorable interactions, glucose is not in the same way affected in blood but is generally taken up and converted in all cell types leading to the short apparent T1.

On the other hand, outside the animal or human body the differences in T1 between these two MCA´s is large (approx. 14s (glucose) versus 60s (pyruvate) subject to specific field strength and temperature. To stand a chance as a clinical MCA it is thus needed to make the time between dissolution and injection as short as possible for glucose. The present paper addresses some of the challenges concerning this time frame. Today it takes, in the clinical setting, approx. 1 min between dissolution from the clinical HP equipment and injection of pyruvate into a patient. This time delay is the result of an evaluation of the injectable (pH, radical removal and transport from the equipment). Glucose is neutral and will not need a pH evaluation; the toxicology profile of the UV radical precursor is not addressed in this paper, but it is no longer a radical when it is injected; the dissolution from a small transport device will allow short proximity to the clinical MR scanner. All of the previous is likely to provide the possibility that glucose may in fact stand a chance to be injected as a highly polarized MCA.

For all these reasons we felt that glucose was the right choice as a demonstration molecule, however we agree with the reviewer that pyruvate may be a better choice when we in a next step will make a demonstration in a clinical setting.

Nevertheless, implementing all these comments into the introduction would be beyond the scope of the manuscript. Therefore, we included the following paragraph after mentioning the kind of sample used in this study:

“Moreover, the shorter liquid state T_1 of glucose compared to pyruvic acid after dissolution, would greatly benefit from quicker handling time prior to injection *in vivo* by reducing as much as possible the distance between the scanner and the dissolution device. This is far from trivial when dissolving the sample directly from the dDNP polarizer.”

Finally, we added the following sentence in the conclusions:

“Finally, we want to draw the attention of the reader to the fact that our new methodology can pave the way towards transportation of HP MCAs in the solid state, dispensing from the presence of a DNP polarizer at individual clinical sites. After transportation, the HP sample still needs to be dissolved. Because of the compact dimension of

the transport/storage device, this operation could be performed on the side of the MRI scanner reducing the handling time of the HP solution. Nevertheless, all dDNP limitations related to the MCAs' relaxation time in solution still stand"

To be absolutely clear: this is an absolute breakthrough for DNP and must be published. But IMHO, please modify the way you present it.

Thanks for your efforts! its an important contribution to the field.

Point-by-point for rev 3

1) Abstract is long and misleading

We rewrote the abstract (see above the response to general comment)

Let's write a more concise abstract

2)line 47, add a comma

OK

3) line 48, replace latter

"Latter" replaced with "These": "These techniques represent powerful means to diagnose and monitor response to therapy.[4]"

4) line 52, glucose is not the golden standard for metabolism in general

We toned down the emphasis on the glucose. Please, see reviewer 2 answer 2.

5) line 59, rephrase glucose downstream metabolism issue in the context of PET

We followed the referee suggestion to remove "since".

6) line 62, what is a phenotypical characterization

We have chosen to delete phenotypical and rewrite the sentence. It now reads: "These techniques allow characterization of tumors by measuring downstream metabolism enabled by good spectral resolution of the different metabolites"

7) line 64, rephrase low sensitivity issue for NMR

"Sensitivity" was replaced with "SNR".

8) line 66, MR signal description not clear and sentence not clear.

We followed the reviewer's suggestion and rephrased as follows

"The MR signal is proportional to the nuclear spins' concentration and polarization (i.e. the net alignment of the nuclear spins ensemble in the direction of the applied magnetic field, the so-called B_0). Because of its gyromagnetic ration, 13C sensitivity is a fourth compared to proton MRS and its natural abundance is only 1 %."

9) line 67, averaging → low temporal resolution not true

We are sorry, but we have to disagree with the reviewer here. Temporal resolution is linked to the repetition time of the NMR sequence: is we acquire 1 FID every 20 s our temporal resolution is 20 s. Indeed, in traditional (non hyperpolarized) 13C MRS, where you have to average to get a decent signal, when investigating a metabolic pathway, you have information about what enters the pathway and what exits the pathway. Therefore, you try to model what happens in between. With hyperpolarized MRS you can "see" what happens in between because you can measure single shot (no average) spectra every e.g. 1s. We agree with the reviewer that averaging does not mean poor spatial resolution, but we did not mention that in the text.

10) line 73, general advancement → correct sentence?

We rephrased the sentence that now reads: Limitations of MRS techniques has benefitted from developments in hyperpolarization technologies.

11) line 74, replace sensitivity with SNR

OK

12) line 75, remove largely

OK

13) line 78, specify "method to hyperpolarize small molecule in solution"

OK

14) line 80, specify field or polarization

We specified clinical scanner 1.5 T – 3 T.

15) line 81, rephrase, too colloquial

We replaced "called" with "known as".

16) line 84, add how the nuclear polarization is achieved

We completed the sentence with "Shining microwaves slightly at a frequency slightly higher or lower with respect to the electron spins resonance (ESR), polarization can be transferred from the electrons to the nuclei, thanks to their dipolar coupling."

17) line 84, is there a connection between long polarization time and short life time

No, it is an observation and most of all a limitation of the technique. We have modified the sentence not to indicate any connection. It now reads: "Whereas, it typically takes hours to create a single injectable dose of MCA, the HP MCA's lifetime is only minutes after dissolution and extraction from the polarizer".

18) line 93, when cooling is the half-life longer also with radical present?

Actually, even in presence of radicals the T1 is much longer when lowering the temperature (look for instance at relaxation times for MAS DNP – 100 K- and dDNP – 1.2 K-). We clarified the sentence including the following: " The ^{13}C polarization's half-life within the MCAs is several orders of magnitude longer when kept frozen at cryogenic temperature, even in presence of radicals."

19) line 101, condense above paragraph

We condensed the paragraph. It now reads: The ^{13}C polarization's half-life within the MCAs is several orders of magnitude longer when kept frozen at cryogenic temperature, even in presence of radicals. This allows, in principle, transportation of the MCAs far away from their production site.[22] Unfortunately, a dDNP sample cannot be extracted as a frozen solid without losing its hyperpolarization.[17,23] The problem is the paramagnetism of the radicals that are added to the sample to allow the DNP process to take place inside the polarizer,[24] which induce nuclear spins relaxation that becomes prohibitively fast at low magnetic field.[25] These are the conditions experienced by an HP sample when lifted far away from the high field of the DNP machine.[22,26,27]

20) line 104, rephrase…too dramatic

We undramatized and rephrased: "Lifting the mandatory presence of technically demanding and costly hardware at individual clinical sites could be realized, instead, if HP MCAs were produced at a central facility for subsequent storage and distribution to the site of action. Such remote production of ^{13}C-labelled MCAs could be envisioned to be much like the way clinical examinations are performed with ^{18}F-FDG PET, where the tracer with a short lifetime is delivered on demand."

21) line 113, sentence sounds colloquial

We modified the sentence as follows: The first approach, proposed by Hirsch et al., does not use DNP to increase the polarization of the substrate of interest. Indeed, no paramagnetic agents are added to the MCA formulation, which is hyperpolarized by brute force (e.g. cooling down the sample to very low temperatures while keeping it at high magnetic field).[26]

22) line 154, make it all is colloquial

We modified the heading as follows: “CFP performance” and shortened the paragraph to show results only (see reviewer 2, comment 5).

23) line 155 to 176, not results

See point 22 and referee 2

24) line 185, please describe what is on the figure

The concerned paragraph was modified and Figure description addressed directly. See point 22 and referee 2.

25) line 205 to 208, rephrase and be more precise with experimental conditions

We modified the paragraph to be more precise and provide only information useful to the understanding of the work (see point 22)

26) line 217, reasoning not clear rephrase

We added the following paragraph to methods (**Microwave delivery and solid-state NMR measurements**): “Relaxation after thermalization was acquired by pulsing every 10 min. These measurements were performed at 4.2 K instead of 1.2 K because even in presence of radicals the relaxation time at 1.2 K can be several hours long, making it difficult to interpret the outcome of the quenching procedure. Differently, at 4.2 K amorphous solids enter a different relaxation regime (from direct process to Raman and Orbach, see Tom Wenckebach book on “Essential of Dynamic Nuclear Polarization”), and the T1 becomes tens of minutes long when radicals are present. In absence of radicals the T1 increases to several hours at 4.2 K, making it straightforward to interpret the outcome of the quenching procedure.”

27) line 221 rephrase the fitting sentence

Thank you for spotting the mistake, we modified the sentence accordingly:

“In Figure S3 we report the results: by fitting a mono-exponential curve to data, we found a T_1 of 4.0±0.5 h (R^2 = 0.97).”

28) line 222, change the heading, it is misleading

We changed it as follows: “**Radical free solid sample extraction**”

29) line 224, rephrase

We followed the reviewer’s suggestion and rewrote the paragraph as follows. All non-essential information was moved to methods:

"**Radical free solid sample extraction**

Despite quenching the radicals prior to HP solid sample extraction reduced the polarization losses from 90 % to 10 %, when exposing it to a magnetic field as small as 40 mT, lower values made the polarization to relax completely (see Figure 4A).

As the above results indicate severe relaxation due to exposure of the sample to a magnetic field lower than 40 mT, we modified the original DNP probe[39] by adding a "permanent magnets rail" providing a magnetic field of least 100 mT and oriented perpendicularly to the polarizer B_0 (see Figure 4B). Details about the magnetic rail construction and magnetic field simulation are reported in the *Methods* section and Figure S5 and S6, respectively.

Repeating the experiment employing the new DNP probe, we were able to move a quenched sample from the polarizer isocenter to the loading chamber while retaining more than 90% of the polarization (see Figure 4C).

It is important to notice that placing permanent magnets inside the DNP probe had no detrimental effects neither on the homogeneity or shift of the NMR resonance nor on the polarizer base temperature, despite potentially increased heat conductivity."

30) line 225, make it more clear

See comment 29.

31) line 236, "most is not precise enough", provide numbers

See comment 29.

32) line 240, please condense the paragraph above

See comment 29.

33) line 242, modify sentence to more informative and concise:

See comment 29.

34) line 239 and 243, move information to methods

OK

35) line 249, redundant

OK. We removed the sentence "to cover the space from 40 cm above the polarizer's isocenter to the loading chamber."

36) line 259, change heading to less colloquial jargon

We modified the heading as follows: "**Sample transport and remote dissolution**"

37) line 266, no results until here

We followed the reviewer suggestion and condensed the paragraph as follows. All other information was moved to methods:

"**Sample transport and remote dissolution**

From field cycling experiments inside the polarizer, it was clear that hours long T_1 could be obtained for [U-^{13}C, d_7]-D-glucose at 1 T and liquid helium temperatures (see above). Since storage in liquid helium requires construction of a cryostat, we obtained the first results at liquid nitrogen temperature in a field of 1 T employing a simple transportation device (see Figure 5A to E and *Methods* for details about the construction of the transportation device).

Disconnecting the loading chamber containing the sample, lowering it into liquid nitrogen inside the storage magnet and reaching a NMR spectrometer placed 50 m far away from the polarizer took approx. 3 min. Once close to the NMR spectrometer, on-site dissolution generated a glucose polarization of 4.0±1.0 %, (n = 4). One last optimization, aiming at speeding up the loading chamber disconnection, concerned the replacement of its vacuum clamp with a quick release one (results reported in Figure 5F). We encourage the reader to watch the video recorded about the hyperpolarization transport and remote dissolution (see Movie S1)."

38) line 271, gate valve is laboratory slang?

We chose to keep the term "gate valve" since this is the technical name on the market for this device.

39) line 277, still no results

See point 37

40) line 279, I suggest to condense the above paragraph and move to methods what it is not results

See point 37

41) line 288, remove "smart"

"smart" was replaced with "new"

42) line 291, remove your motivation

We removed the sentence.

43) line 318, can you condense the previous paragraph?

Although being concise is important, we think that an exhaustive discussion about the polarization losses is crucial. Nevertheless, we tried to polish the text to the best of our capability. Now the paragraph reads:

"We characterized one source of relaxation in the experiment. The UV-radicals quenching process accounts for a relative polarization loss of 20%. This would project the maximum achievable liquid-state ^{13}C polarization for glucose to 24%. According to the data reported in Figure 4B, lifting a UV-radical quenched sample to the loading chamber causes almost no loss of polarization.

Moreover, if the gate valve was opened and the sample subjected to the cold He gas stream, performing a fast extraction (10 s) compared to a slow one (approx. 2 min) did not make any difference."

44) line 325, what value of T1

We specified the sentence by indicating clearly the value of T1 we estimate (i.e. 5 min at 77 K and 1 T)

45) line 328, comment on how to measure signal loss due to heating during docking

Although, running a series of experiments, it could be possible to estimate this loss e.g. by leaving the sample into the loading chamber, for increasing time intervals followed by dissolution and measurement in the liquid state, this would not represent a sufficiently controlled experimental environment. To answer this question, we chose to implement NMR measurements inside the transportation device. This will be the subject of a future study.

46) line 334, specify experimental conditions

We specified the conditions as in the following text: "To provide conditions for longer storage and/or transport, a colder environment is needed (i.e. below 4.2 K). At liquid He temperature, hours long T_1 can be obtained"

47) line 373, redundant sentence

OK. We removed the sentence. Now the paragraph writes:

"Finally, we want to stress that even in the ideal case of complete absence of paramagnetic impurities in the sample, for a magnetic field value < 40 mT ^{13}C and ^{1}H nuclei are subjected to "low-field thermal mixing".[22,27]"

REVIEWERS' COMMENTS:

Reviewer #3 (Remarks to the Author):

Many thanks for addressing the comments, and congratulations to your great work.